Notes, Mathematical Cell Biology Course

Leah Edelstein-Keshet

May 2, 2012

Contents

Chapter 1

Qualitative behaviour of simple ODEs and bifurcations

1.0.1 Cubic kinetics

We now consider an example where there are three steady states. Here is one of the most basic examples exhibiting bistability of solutions.

$$\frac{dx}{dt} = c\left(x - \frac{1}{3}x^3\right) \equiv f(x), \quad c > 0 \text{ constant.} \tag{1.1}$$

(The factor 1/3 that multiplies the term in (1.1) is chosen to slightly simplify certain later formulas. Its precise value is not essential. In Exercise 4.6a we found that Eqn. (1.1) can be obtained by rescaling a more general cubic kinetics ODE.

We graph the function $f(x)$ for Eqn. (1.1) in Fig 1.1(a). Solving for the steady states of (1.1) $(dx/dt = f(x) = 0)$, we find that there are three such points, one at $x = 0$ and others at $x = \pm\sqrt{3}$. These are the intersections of the cubic curve with the x axis in Fig. 1.1(a). By our usual techniques, we surmise the direction of flow from the sign (positive/negative) of $f(x)$, and use that sketch to conclude that $x = 0$ is unstable while both $x = -\sqrt{3}$ and $x = \sqrt{3}$ are stable. We also note that the constant c does not affect these conclusions. (See also Exercise 1.**??**.) In Fig. 1.1(b), we show numerically computed solutions to Eqn. (1.1), with a variety of initial conditions. We see that all positive initial conditions converge to the steady state at $x = +\sqrt{3} \approx 1.73$, whereas those with negative initial values converge to $x = -\sqrt{3} \approx -1.73$. Thus, the outcome depends on initial conditions in this problem. We will see other example of such **bistable kinetics** in a number of examples in this book, with a second appearance of this type in Section 1.0.2.
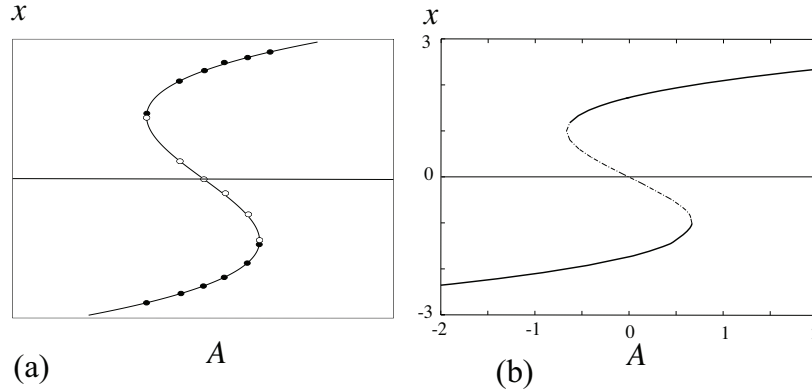
Figure 1.4. *(a) Here we have removed flow lines from Fig. 1.3b and rotated the diagram. The vertical axis is now the x axis, and the horizontal axis represents the value of the parameter A. (b) A bifurcation diagram produced by XPPAUT for the differential equation 1.1. The thick line corresponds to the black dots and the thin lines to the white dots in (a). Note the resemblance of the two diagrams. As the parameter A varies, the number of steady states changes. See Appendix A.B.1 for the XPP file and instructions for producing (b).*

We now consider the revised equation

$$\frac{dx}{dt} = c\left(x - \frac{1}{3}x^3 + A\right) \equiv f(x). \tag{1.2}$$

where A is some additive constant, which could be either positive or negative. Without loss of generality, we can set $c = 1$, since time can be rescaled as discussed in Exercise 4.6b.

Clearly, A shifts the location of the cubic curve (as shown in Fig 1.3a) upwards ($A > 0$) or downwards ($A < 0$). Equivalently, and more easily illustrated, we could consider a fixed cubic curve and shift the x axis down ($A > 0$) or up ($A < 0$), as shown in 1.3b. As A changes, so do the positions and number of intersection points of the cubic and the x axis. For certain values of A (not too large, not too negative) there are three intersection points. We have colored them white or black according to their stability. If A is a large positive value, or a large negative value, this is no longer true. Indeed, there is a value of A in both the positive and negative directions beyond which two steady states coalesce and disappear. This type of change in the qualitative behaviour is called a **bifurcation**, and A is then called a **bifurcation parameter**.

We can summarize the behaviour with a **bifurcation diagram**. The idea is to represent the number and relative positions of steady states (or more complicated attractors, as we shall see) versus the bifurcation parameter. It is customary to use the horizontal axis for the parameter of interest, and the vertical axis for the steady states corresponding to that parameter value. Consequently, to do so, we will suppress the flow and arrows on Fig 1.3b, and rotate the figure to show only the steady state values. The result is Fig 1.4(a). The parameter A that was responsible for the shift of axes in Fig. 1.3b is now along the

horizontal direction of the rotated figure. We have thereby obtained a bifurcation diagram. In the case of the present example, which is simple enough, we can calculate the values of A at which the bifurcations take place (**bifurcation values**). In Exercise 1.3, we guide the reader in determining those values, A_1 and A_2. (See, in particular, the configurations shown in Fig 1.10.)

In general, it may not be possible to find bifurcation points analytically. In most cases, software is used to follow the steady state points as a parameter of interest is varied. Such techniques are commonly called **continuation methods**. XPP has this option as it is linked to Auto, a commonly used, if somewhat tricky package [1]. As an example, Fig. 1.4(b), produced by XPP auto for the bifurcation in (1.2) is seen to be directly comparable to our result in Fig. 1.4(a). The solid curve corresponds to the stable steady states, and the dashed part of the curve represents the unstable steady states. Because this bifurcation curve appears to fold over itself, this type of bifurcation is called a **fold bifurcation**. Indeed, Fig. 1.4 shows that the cubic kinetics (1.2) has two fold bifurcation points, one at a positive, and another at a negative value of the parameter A.

Bistability is accompanied by an interesting **hysteresis** as the parameter A is varied. In Fig. 1.5, we show this idea. Suppose we start the system with a negative value of A in the lowest (negative) steady state value. Now let us gradually increase A. We remain at steady state, but the value of that steady state shifts, moving rightwards along the lower branch of the S in Fig. 1.5. At the bifurcation value, the steady state disappears, and a rapid transition to the high (positive) steady state value takes place. Now suppose we decrease A back to lower values. We remain at the elevated steady state moving left along the upper branch until the lower (negative) bifurcation value of A. This type of hysteresis is often used as an experimental hallmark of multiple stable states and bistability in a biological system.

1.0.2 Bistability

A common model encountered in the literature is one in which a sigmoidal function (often called a Hill function) appears together with first order kinetics, in the following form:

$$\frac{dx}{dt} = f(x) = \frac{x^2}{1+x^2} - mx + b \tag{1.3}$$

where $m, b > 0$ are constants. Here the **Hill function** (first rational term in Eqn. (1.3)) has "Hill constant" $n = 2$, but similar behaviour is obtained for $n \geq 2$. This equation is remarkably popular in modeling of switch-like behaviour. As we will see in Chapter **??**, equations of a similar type are obtained in chemical processes that involve cooperative kinetics, such as formation of dimers and their mutual binding. Another example is the behaviour of a hypothesized chemical in an old but instructive model of morphogenesis in [13].

Here we investigate only the caricature of such systems, given in (1.3), noting that the first term could be a rate of autocatalysis production of x, b a source or production term (similar to the parameter I in Eqn. (**??**)), and m the decay rate of x (similar to the parameter γ in Eqn. (**??**)). The simplest case to be analyzed here, is $b = 0$. Then we can easily solve for the steady states of this equation. In the case $b = 0$, one of the steady states of (1.3) is

$x = 0$, and two others satisfy

$$\frac{x^2}{1+x^2} - mx = 0, \quad \Rightarrow \quad \frac{x}{1+x^2} = m, \quad \Rightarrow \quad x = m(1+x^2).$$

Simplification and use of the quadratic formula leads to the result

$$x_{ss1,2} = \frac{1 \pm \sqrt{1-4m^2}}{2m} \tag{1.4}$$

[Exercise 1.4]. Clearly there are two possible values ($\pm$), but these steady states are real only if $m < 1/2$.

Let us sketch the two parts of $f(x)$, i.e. the sigmoid $y = x^2/(1+x^2)$ and the straight line $y = mx$ on the same plot, as shown in Fig. 1.6. In the case $m > 1/2$ (dashed line) only one intersection, at $x = 0$ is seen. For $m < 1/2$ there are three intersections (solid line). Separating these two regimes is the value $m = 1/2$ at which the line and sigmoidal curves are tangent. This is the **bifurcation value** of the parameter m.

1.0.3 Other bifurcations

Many simple differential equations illustrate interesting bifurcations. We mention here for completeness the following examples, and leave their exploration to the reader. A more complete treatment of such examples is given in [16]. In all the following examples, the bifurcation parameter is r and the bifurcation value occurs at $r = 0$.

A simpler example of a **fold bifurcation**, also called **saddle-node bifurcation** is illustrated in the ODE

$$\frac{dx}{dt} = f(x) = r + x^2. \tag{1.5}$$

We see from this equation that steady states are located at points satisfying $r + x^2 = 0$, namely at $x_{ss} = \pm\sqrt{-r}$. These two values are real only when $r < 0$. When $r = 0$, the values coalesce into one and then disappear for $r > 0$. We show the qualitative portrait for Eqn. (1.5) in Fig. 1.7(a), and a sketch of the bifurcation diagram in panel (b).

A **transcritical bifurcation** is typified by:

$$\frac{dx}{dt} = rx - x^2. \tag{1.6}$$

This time, we demonstrate the use of XPPAUT in the bifurcation diagram of Fig. 1.8. A stable steady state (solid line) coexists with an unstable steady state (dashed line), they meet and exchange stability at the bifurcation value $r = 0$. Exercise 1.8 further explores details of the dynamics of (1.6) and how these correspond to this diagram.
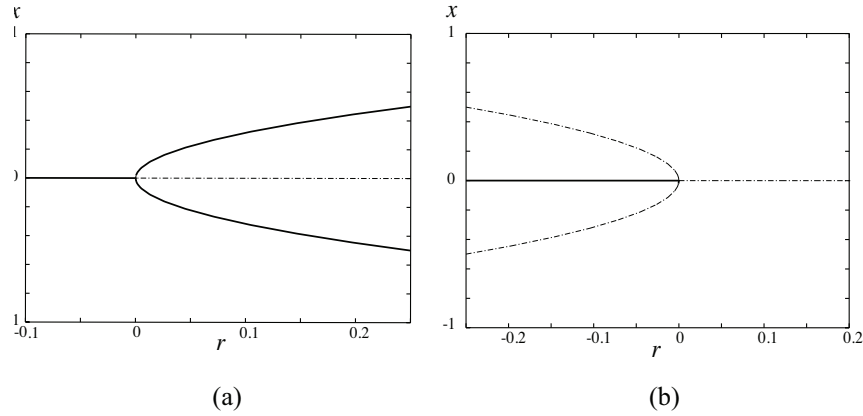
(a)   (b)

Figure 1.9. *(a) Pitchfork bifurcation exhibited by Eqn. (1.7) as the parameter r varies from negative to positive values. For r < 0 there is a single stable steady state at x = 0. At the bifurcation value of r = 0, two new stable steady states appear, and x = 0 becomes unstable. (b) A subcritical pitchfork bifurcation that occurs in (1.8). Here the two outer steady states are unstable, and the steady state at x = 0 becomes stable as the parameter r decreases. Diagrams were produced with the XPP codes in Appendix A.B.2.*

The **pitchfork bifurcation** is illustrated by the equation:

$$\frac{dx}{dt} = rx - x^3. \tag{1.7}$$

See Fig 1.9(a) for the bifurcation diagram and Exercise 1.9 for practice with qualitative analysis of this equation. We note that there can be up to three steady states. When the parameter r crosses its bifurcation value of $r = 0$, two new stable steady states appear.

A **subcritical pitchfork bifurcation** is obtained in the slightly revised equation,

$$\frac{dx}{dt} = rx + x^3. \tag{1.8}$$

See Fig. 1.9(b) for the bifurcation diagram and Exercise 1.10 for more details.

Exercises

1.1. Consider $dA/dt = aA - a_1A^3$; $a > 0$, $a_1 > 0$. Show that $A = \sqrt{(a/a_1)}$ is a stable steady state.

1.2. Consider $y = f(x) = c(x - \frac{1}{3}x^3 + A)$ as in Eqn .(1.2). Compute the first and second derivatives of this function. Find the extrema (critical points) by solving $f'(x) = 0$. Then classify those extrema as local maxima and local minima using the second derivative test. [Recall that $f''(p) < 0 \Rightarrow$ local maximum, $f''(p) > 0 \Rightarrow$ local minimum, and $f''(p) = 0 \Rightarrow$ test inconclusive.]

1.3. As shown in the text, Eqn. (1.2) undergoes a change in behaviour at certain values of the parameter A. In this exercise we calculate those values. In Fig 1.10, we show two configurations for which the cubic curve intersects the x axis in only two places. If A increases beyond the higher value (or decreases beyond the lower value) only one steady state remains. Note that at these **bifurcation points**, the local maximum (minimum) of the cubic curve just touches the x axis. Use this fact to compute the two values A_1, A_2 at the bifurcations.

1.4. Consider the bistable kinetics described by Eqn. (1.3) and $b = 0$.

(a) Show that aside from $x = 0$, this equation has two steady states given by (1.4). (Hint: show that you obtain a quadratic equation by setting $dx/dt = 0$ and simplifying algebraically.)

(b) What happens to the results obtained in part (a) for the value $m = 1$? for $m = 1/2$?

(c) Compute $f'(x)$ and use this to show that $x = 0$ is a stable steady state.

(d) Use Fig. 1.6 to sketch the flow along the x axis for the following values of the parameter m: $m = 1, 1/2, 1/4$.

(e) Adapt the XPP file provided in Appendix A.B.1 for the ODE (1.3) and solve this equation with $m = 1/4$ starting from several initial values of x. Show that you obtain bistable behaviour, i.e., that there are two possible outcomes, depending on initial conditions.

1.5. Consider again Eqn. (1.3) but now suppose that the source term $b \neq 0$.

(a) Interpret the meaning of this parameter and explain why it should be positive.

(b) Make a rough sketch analogous to Fig. 1.6 showing how a positive value of b affects the conclusions. What happens to the steady state formerly at $x = 0$?

(c) Simulate the dynamics of Eqn. (1.3) using the XPP file developed in Exercise 1.4e for $b = 0.1, m = 1/3$. What happens when b increases to 0.2?

1.6. Consider the model by Ludwig, Jones and Holling [9] for spruce budworm, $B(t)$. Recall the differential equation proposed by these authors, (see also Exercise 4.7.)

$$\frac{dB}{dt} = r_B B \left(1 - \frac{B}{K_B} \right) - \beta \frac{B^2}{\alpha^2 + B^2} \qquad (1.9)$$

where $r_B, K_B, \alpha > 0$ are constants.

(a) Show that $B = 0$ is an unstable steady state of this equation.

(b) Sketch the two functions $y = r_B B \left(1 - \frac{B}{K_B} \right)$ and $y = B^2/(\alpha^2 + B^2)$ on the same coordinate system. Note the resemblance to the sketch in Fig. 1.6, but the straight line is replaced by a parabola opening downwards.

(c) How many steady states (other than the one at $B = 0$) are possible?

1.7. Consider the equation

$$\frac{dx}{dt} = f(x) = r - x^2.$$

Show that this equation also has a fold bifurcation and sketch a figure analogous to Fig. 1.7 that summarizes its behaviour.

1.8. Eqn. (1.6) has a transcritical bifurcation. Plot the qualitative sketch of the function on the RHS of this equation. Solve for the steady states explicitly and use your diagram to determine their stabilities. Explain how your results for both $r < 0$ and $r > 0$ correspond to the bifurcation diagram in Fig. 1.8.

1.9. Consider Eqn. (1.7) and the effect of varying the parameter r. Sketch the kinetics function (RHS of the differential equation (1.7)) for $r > 0$ indicating the flow along the x axis, the positions and stability of steady states. Now show a second sketch with all these features for $r < 0$. Connect your results in this exercise with the bifurcation diagram shown in Fig 1.9(a).

1.10. Repeat the process of Exercise 1.9, but this time for the subcritical pitchfork equation, (1.8). Compare your findings with the bifurcation diagram shown in Fig 1.9(b).

(a)   (b)
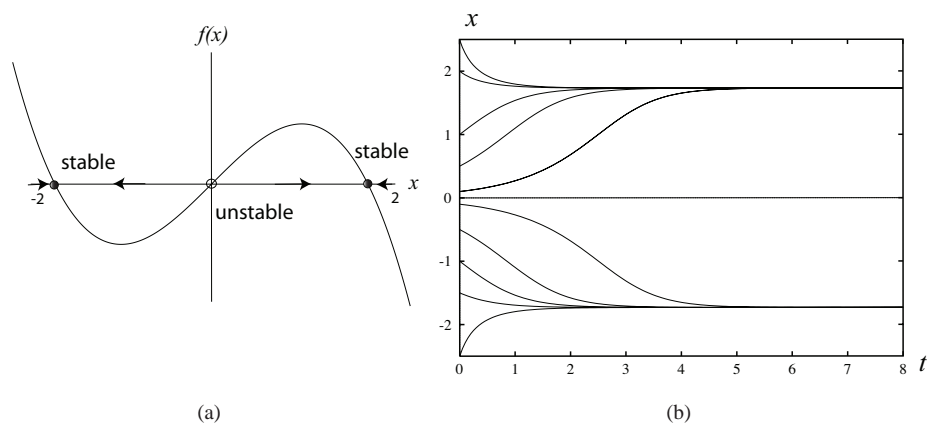
Figure 1.1. *(a) A plot of the function $f(x)$ on the right hand side of the differential equation* (1.1)*. (b) Some numerically computed solutions of* (1.1) *for a variety of initial conditions.*
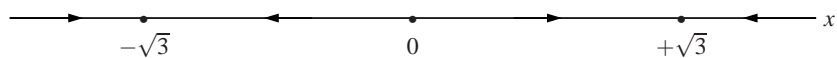

Figure 1.2. *The "phase line" for equation* (1.1)*. Steady states are indicated by heavy points, trajectories with arrows show the direction of "flow" as t increases.*
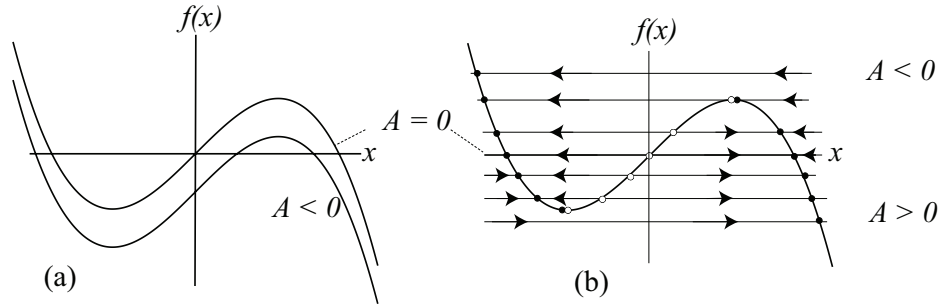
Figure 1.3. *When the parameter A in Eqn. (1.2) changes, the positions of the steady states also change. (a) Here we show the cubic curve for $A = 0$ and $A < 0$. (When A changes, the curve shifts up or down relative to the x axis). (b) Shown here is the flow along the x axis. Same idea as (a), but the x axis is shifted up/down and the cubic curve is drawn once. The height of the horizontal line corresponds to the value of $-A$. Intersections of the x axis and the cubic curve are steady states. (Un)stable steady states are indicated with (white) black dots. Note that there is an abrupt loss of two steady states when A gets large and positive or large and negative.*
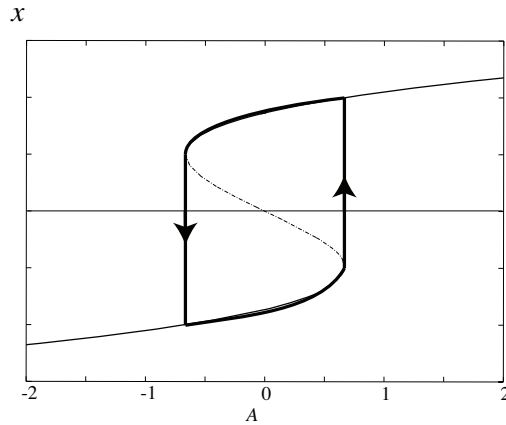
Figure 1.5. *Bistability and hysteresis in the behaviour of the cubic kinetics (1.2). Suppose initially $A = -0.7$ If the parameter is increased, the steady state on the lower (solid) branch of the diagram gradually becomes more positive. Once A reaches the value at the knee of that branch (a fold bifurcation), there is a sudden transition to the higher (positive) steady state value. If the value of A is then decreased, the system takes a different path to its original location.*
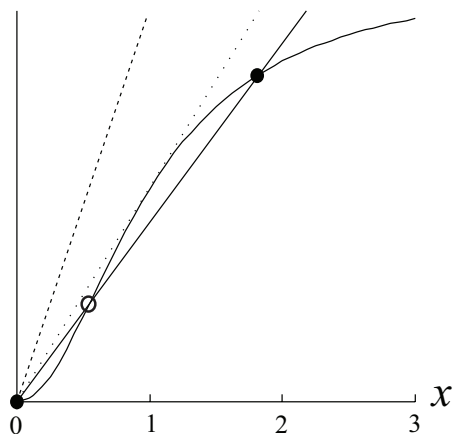
Figure 1.6. *We plot the Hill function and the straight line $y = mx$ here to illustrate their intersections. Steady states of Eqn.* (1.3) *at located at these intersections. A very similar argument is used later in Fig 2.8 to understand how bistability arises in a more complicated equation with a biological interpretation.*
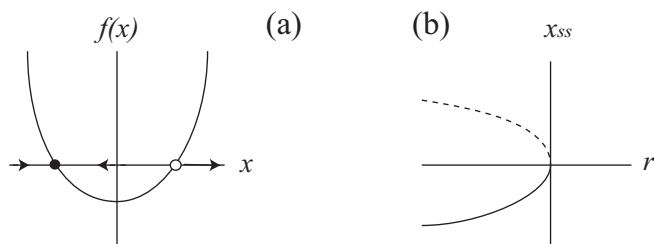
Figure 1.7. *A fold (or saddle-node) bifurcation that occurs in Eqn.* (1.5)*. (a) The qualitative sketch of the function $f(x)$ on the RHS of the equation, showing the positions and stability of the steady states. (Black dot signifies stable, and white dot unstable steady states.) (b) A schematic sketch of the bifurcation diagram which is a plot of the steady state values as a function of the bifurcation parameter r. Solid curve: stable steady state. dashed curve: unstable steady state.*
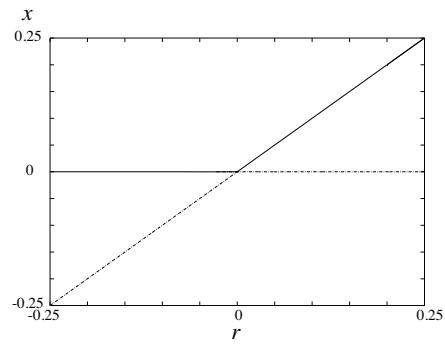
Figure 1.8. *A transcritical bifurcation that occurs in Eqn.* (1.6). *Diagram produced by XPP file in Appendix A.B.3.*
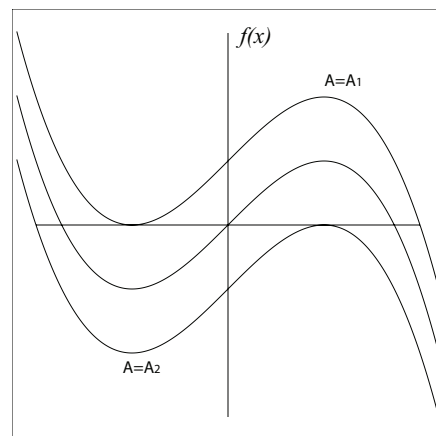
Figure 1.10. *For the differential equation 1.2, there are values of the parameter A that result in a change of behaviour, as two of the steady states merge and vanish.*

Chapter 2

Biochemical modules
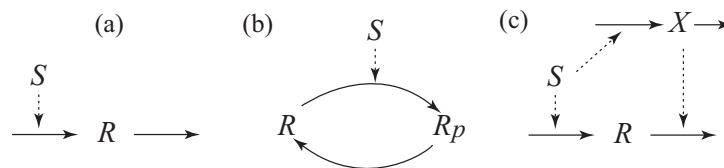
Figure 2.1. *(a) Production and decay of substance R depends on presence of signal S, as shown in Eqn. (2.1). (b) Activation and inactivation (e.g. by phosphorylation and dephosphorylation) of R in response to signal S. The transitions are assumed to be linear in (2.2) and Michaelian in (2.3). (c) An adaptation circuit. Based on [18].*

2.1 Simple biochemical circuits with useful functions

Biochemical circuits can serve as functional modules, much like parts of electrical wiring diagrams. Many of the more complicated models for biological gene networks or protein networks have been assembled by piecing together the performance of smaller modules. See [18], also [7]. Other current papers at the research level include [6, 10, 15, 14].

2.1.1 Production in response to a stimulus

We consider a network in which protein is synthesized at some basal rate k_0 that is enhanced by a stimulus (rate $k_1 S$) and degraded at rate k_2 (Fig 2.1a). Then

$$\frac{dR}{dt} = k_0 + k_1 S - k_2 R. \tag{2.1}$$
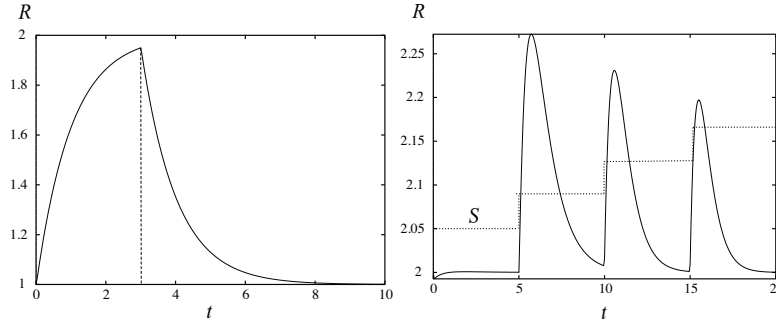
Figure 2.2. *(a) Simulation of simple production-decay of Eqn.* (2.1) *in response to signal that turns on at time* $t = t_1 = 0$ *and off at time* $t = t_2 = 3$. *See XPP file in Appendix A.G.1. (b) Response of the adaptation circuit of* (2.8). *See XPP file in Appendix A.G.2. Note that in part (a) R returns to baseline only* after the signal is turned off, *whereas in (b) R returns to its steady state level even though the signal strength is stepped up at* $t = 0, 5, 10, 15$. *(Signal strength increases in unit steps, not here shown to scale.)*

2.1.2   Activation and inactivation

In Fig 2.1b, R and R_p denote the levels of inactive and active form of the protein of interest, respectively. Suppose that all the processes shown in that figure operate at constant rates. In that case, the equation for the phosphorylated form, R_p takes the form

$$\frac{dR_p}{dt} = k_1 SR - k_2 R_p. \tag{2.2a}$$

Here the first term is the signal-dependent conversion of R to R_p, and k_2 is the rate of the reverse reaction. Conservation of the total amount of the protein R_T, implies that

$$R_T = R + R_p = \text{ constant.} \tag{2.2b}$$

We assume Michaelis-Menten kinetics

$$\frac{dR_p}{dt} = \frac{k_1 SR}{K_{m1} + R} - \frac{k_2 R_p}{K_{m2} + R_p}. \tag{2.3}$$

Here the first term is activation of R when the stimulus S is present. (If $S = 0$ it is assumed that there is no activation.) The second term is inactivation. Using the conservation (2.2b) we can eliminate R and recast this equation in the form

$$\frac{dR_p}{dt} = \frac{k_1 S(R_T - R_p)}{K_{m1} + (R_T - R_p)} - \frac{k_2 R_p}{K_{m2} + R_p}. \tag{2.4}$$

If we express the active protein as fraction of total amount, e.g. $r_p = R_p/R_T$ then Eqn. (2.4) can be rescaled to

$$\frac{dr_p}{dt} = \frac{k_1 S(1 - r_p)}{K'_{m1} + (1 - r_p)} - \frac{k_2 r_p}{K'_{m2} + r_p}. \tag{2.5}$$

Figure 2.3. *(a) A plot of each of the two terms in Eqn.* (2.5) *as a function of r_p assuming constant signal S. Note that one curve increases from $(0,0)$ whereas the other curve decr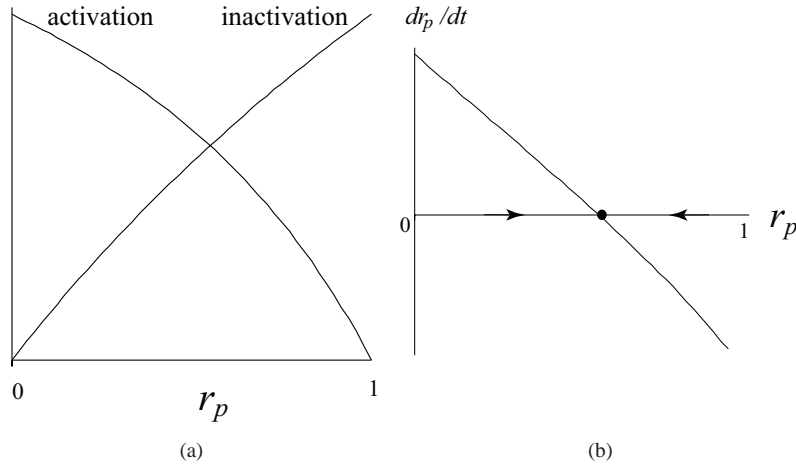eases to $(1,0)$, and hence there is only one intersection in the interval $0 \leq r_p \leq 1$. (b) The difference of the two curves in (a). This is a plot of dr_p/dt and allows us to conclude that the single steady state in $0 \leq r_p \leq 1$ is stable.*

Steady state(s) of (2.5) satisfy a quadratic equation. This suggests that there could be two steady states, but as it turns out, only one of these need concern us, as the argument below demonstrates.

How does the steady state value of the response depend on the magnitude of the signal? let $u = k_1 S, v = k_2, J = K_{m1}, K = K_{m2}$. Note that the quantity u is proportional to the signal S, and we will be interested in the steady state response as a function of u. Then solving for the steady state of (2.5) reduces to solving an equation of the form

$$\frac{u(1-x)}{J+1-x} = \frac{vx}{K+x}, \quad \text{where } x \equiv r_p. \tag{2.6}$$

In the exercises, we ask the reader to show that this equation reduces to a quadratic

$$ax^2 + bx + c = 0, \quad \text{where} \quad a = (v-u), \ b = u(1-K) - v(1+J), \ c = uK. \tag{2.7}$$

We can write the dependence of the scaled response, $r_p = x$ on scaled signal, u. The result is function $r_p(u)$ that Tyson denotes the "Goldbeter-Koshland function". (As this function is slightly messy, we relegate the details of its form to Exercise 2.3.) We can plot the relationship to observe how response depends on signal. To consider a case where the enzymes operate close to saturation, let us take $K = 0.01, J = 0.02$. We let $v = 1$ arbitrarily and plot the response r_p as a function of the "signal" u. We obtain the shape shown in Fig 2.4. The response is minimal for low signal level, until some threshold around $u \approx 1$. There is then a steep rise, when u is above that threshold, to full response $r_p \approx 1$. The change from no response to full response takes place over a very small increment in signal strength, i.e. in the range $0.8 \leq u \leq 1.2$ in Fig. 2.4. This is the essence of a "zero order ultrasensitivity" switch. More details for further study of topic are given in Section **??**.
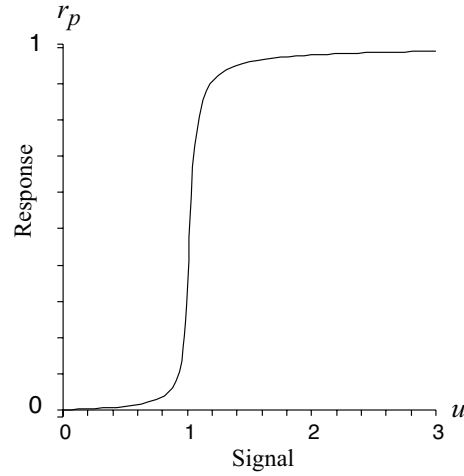
Figure 2.4. *Goldbeter Koshland "zero order ultrasensitivity". Here u represents a stimulus ($u = k_1 S$) and r_p is the response, given by a (positive) root of the quadratic equation (2.7). As the figure shows, the response is very low until some threshold level of signal is present. Thereafter the response is nearly 100% on. Near the threshold (around $u = 1$) it takes a very small increase of signal to have a sharp increase in the response.*

2.1.3 Adaptation

Cells of the social amoebae *Dictyostelium discoideum* can sense abrupt increases in their chemoattractant (cAMP) over a wide range of absolute concentrations. In order to sense *changes*, the cells exhibit a transient response, and then gradually **adapt** if the cAMP level no longer changes.

A circuit shown in Fig. 2.1c consists of an additional chemical, denoted by X that is also made in response to signal at some constant rate. However, X is assumed to have an inhibitory effect on R, i.e. to enhance its turnover rate. The simplest form of such a model would be

$$\frac{dR}{dt} = k_1 S - k_2 X R, \tag{2.8a}$$

$$\frac{dX}{dt} = k_3 S - k_4 X. \tag{2.8b}$$

Behaviour of (2.8) is shown in response to a changing signal in Fig. 2.2(b). After each step up, the system (2.8) reacts with a sharp peak of response, but that peak rapidly decays back to baseline. Adaptation circuits of a similar type have been proposed by Levchenko and Iglesias [8, 5] in extended spatial models of gradient sensing and adaptation in *Dictyostelium discoideum*. In that context, they are known as **local excitation global inhibition** (LEGI) models. Such work has engendered a collection of experimental approaches aimed at understanding how cells detect and respond to chemical gradients, while adapting to uniform elevation of the chemical concentration.

2.2 Genetic switches

A simple switch genetic switch was devised by the group of James Collins [3] using an artificially constructed pair of mutually inhibitory genes (transfected via plasmids into the bacterium *E. coli*). Here each of the gene products acts as a repressor of the second gene. We examine this little genetic circuit here.
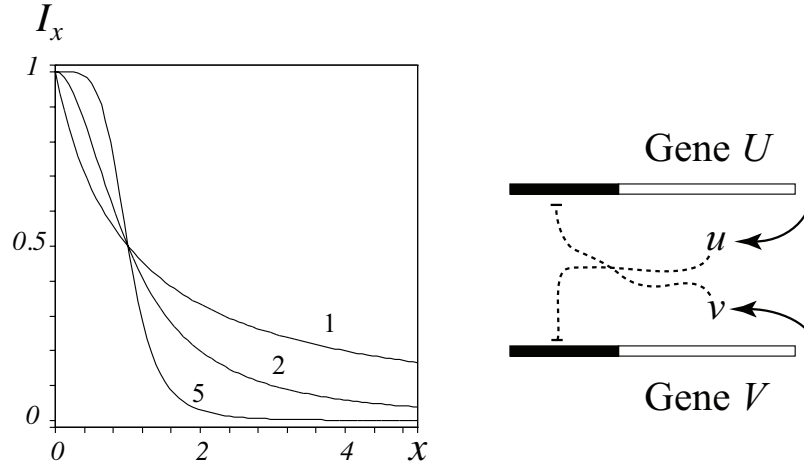
Figure 2.5. *Right: The construction of a genetic toggle switch by Gardner et al [3], who used bacterial plasmids to engineer this circuit in a living cell. Here the two genes, U,V produce products u,v, respectively, each of which inhibit the opposite gene's activity. (Black areas represent the promotor region of the genes.) Left: a few examples of the functions* (2.10) *used for mutual repression for n = 1,2,5 in the model* (2.11). *Note that these curves become more like an on-off switch for high values of the power n.*

Let us denote by u the product of one gene (U), and v the product of gene V. Each product is a protein with some (relatively fixed) lifetime, i.e. degradation at constant rate causes removal of each protein. Suppose for a moment that both genes are turned on and not coupled to one another. In that case, we would expect their product to satisfy the pair of equations

$$\frac{du}{dt} = I_u - d_u u, \tag{2.9a}$$

$$\frac{dv}{dt} = I_v - d_v v. \tag{2.9b}$$

Here I_u, I_v are rates of production that depend on gene activity for genes U, V respectively, and d_u, d_v are the decay rates.

Now let us recraft the above to include the repression of each product on the other's gene activity. We can do so by an assumption that production of a given product decreases
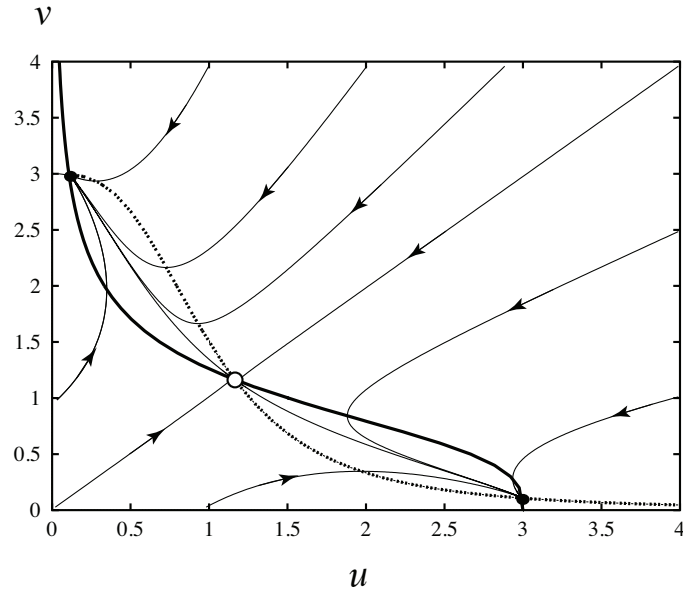
Figure 2.6. *Phase plane behaviour of the toggle switch model by Gardner et al [3], given by Eqs. (2.11) with $\alpha_1 = \alpha_2 = 3, n = m = 3$. See XPP file in Appendix A.G.3. The two steady states close to the u or v axes are stable. The one in the center is unstable. The nullclines are shown as the dark solid curve (u nullcline) and the dotted curve (v nullcline).*

due to the presence of the other product. Gardner et al [3] assumed terms of the form

$$I_x = \frac{\alpha}{1 + x^n}. \tag{2.10}$$

We plot a few curves of type (2.10) for $\alpha = 1$ and various values of the power n. This family of curves intersect at the point $(0,1)$. For $n = 1$ the curve decreases gradually as x increases. For larger powers (e.g. $n = 2, n = 5$), the curve has a little "shoulder", a steep portion, and a much flatter tail, resembling the letter "Z".

Gardner et al [3] employed the following equations (wherein d_u, d_v were arbitrarily taken as unit rates.)

$$\frac{du}{dt} = \frac{\alpha_1}{1 + v^n} - u, \tag{2.11a}$$

$$\frac{dv}{dt} = \frac{\alpha_2}{1 + u^m} - v. \tag{2.11b}$$

The behaviour of this system is shown in the phase plane of Fig. 2.6. The presence of two stable steady states is a hallmark of **bistability**,.
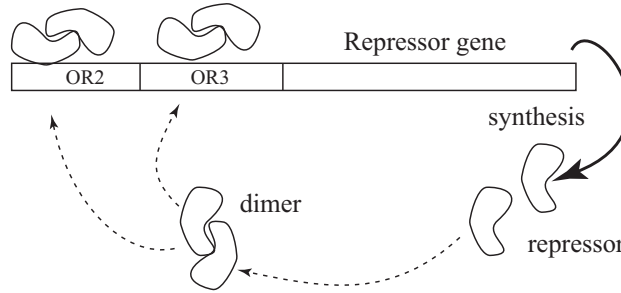
Figure 2.7. *The phage λ gene encodes for a protein that acts as the gene's repressor. The synthesized protein dimerizes and the dimers bind to regulatory sites (OR2 and OR3) on the gene. Binding to OR2 activates transcription, whereas biding to OR3 inhibits transcription.*

2.3   Dimerization in a genetic switch: the λ virus

Dimerization is a source of cooperativity that frequently appears as a motif in regulation of gene transcription[1]. Here we illustrate this idea with the elegant model of Hasty et al [4] for the regulation of a gene and its product in the λ virus.

The protein of interest is transcribed from a gene known as cI (schematic in Fig. 2.7) that has a number of regulatory regions. Hasty et al consider a mutant with just two such regions, labeled OR2 and OR3. The protein synthesized from this gene transcription dimerizes, and the dimer acts as a regulator, i.e. **transcription factor** for the gene. Binding of dimer to the OR2 region of DNA activates gene transcription, whereas biding to OR3 stops transcription.

We follow the notation in [4], defining X as the repressor, X_2 a dimerized repressor complex, D the DNA promotor site. The fast reactions are the dimerization and binding of repressor to the promotor sites OR2 and OR3, for which the chemical equations are taken as

$$\text{Dimerization:} \qquad 2X \underset{}{\overset{K_1}{\rightleftharpoons}} X_2$$

$$\text{Binding to DNA (OR2):} \quad D + X_2 \underset{}{\overset{K_2}{\rightleftharpoons}} DX_2$$

$$\text{Binding to DNA (OR3):} \quad D + X_2 \underset{}{\overset{K_3}{\rightleftharpoons}} DX_2^*$$

$$\text{Double binding (OR2 and OR3):} \quad DX_2 + X_2 \underset{}{\overset{K_4}{\rightleftharpoons}} DX_2X_2 \qquad (2.12\text{a})$$
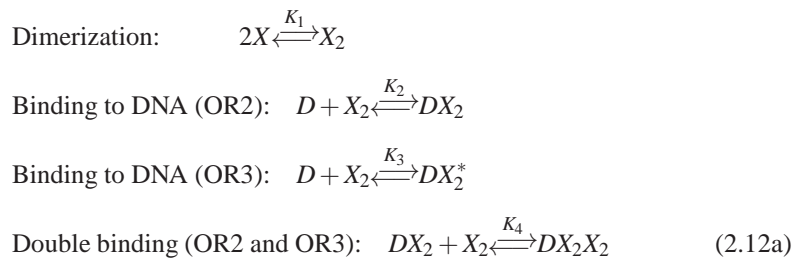
Here the complexes DX_2, DX_2^* are, respectively, the dimerized repressor bound to site OR2 or to OR3, and DX_2X_2 is the state where both OR2 and OR3 are bound by dimers.

On a slower timescale, the DNA is transcribed to produce n copies of the gene product

---

[1]I wish to acknowledge Alex van Oudenaarden, MIT, whose online lecture notes alerted me to this very topical example of dimerization and genetic switches.

(a)   (b)
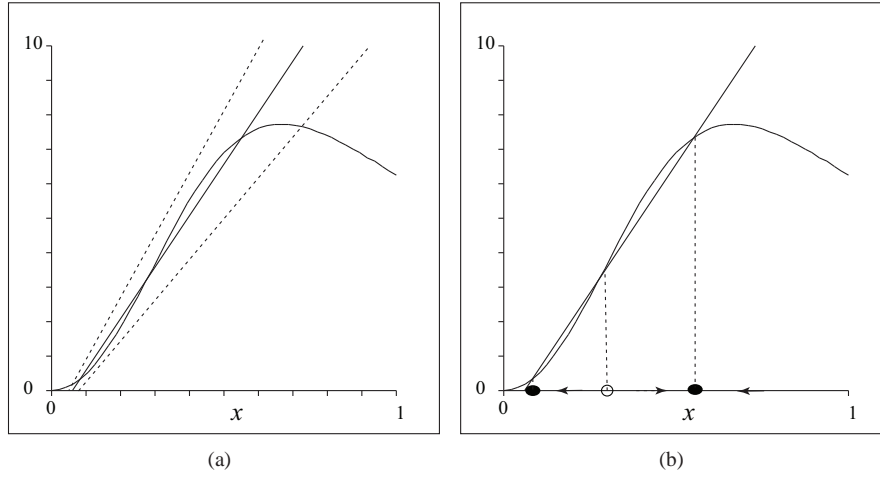
Figure 2.8. *(a) A plot of the two functions given by Eqs.* (2.16) *for the simplified dimensionless repressor model* (2.15). *(lowest dashed line:)* $\gamma = 12$, *(solid line:)* $\gamma = 14$, *and (highest dashed line:)* $\gamma = 18$. *(b) For* $\gamma = 14$, *we show the configuration of the two curves and the positions of the resultant three steady states. The outer two are stable and the intermediate one is unstable. Compare this figure with Fig. 1.6 where a similar argument was used to understand the bifurcation structure of a simpler model involving a straight line and a Hill function.*

and the repressor is degraded. The chemical equations for these are taken to be

$$\text{Protein synthesis:} \quad DX_2 + P \xrightarrow{k_1} DX_2 + P + nX$$

$$\text{Protein degradation:} \quad X \xrightarrow{k_d} A \tag{2.12b}$$
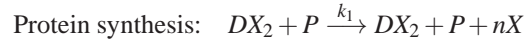
We define variables as follows: x, y are the concentrations of X, X_2, respectively, and d, u, v are the concentrations of D, DX_2, DX_2^*. Similarly, z is the variable for DX_2X_2. The full set of kinetic equations for this system are the topic of Exercise 2.8. However, u, v, y, z are variables that change on a fast timescale, and a QSS approximation is applied to these. Because the total amount of DNA is constant, there is a conservation equation,

$$d_{total} = d + u + v + z. \tag{2.13}$$

We ask the reader [Exercise 2.8] to show that, based on the QSS approximation for the fast variables, the equation for x simplifies to the form

$$\frac{dx}{dt} = \frac{AK_1K_2x^2}{1 + (1+\sigma_1)K_1K_2x^2 + \sigma_2K_1^2K_2^2x^4} - k_dx + r, \tag{2.14}$$

where A is a constant. This can be rewritten in dimensionless form by rescaling time and x appropriately to arrive at

$$\frac{dx}{dt} = \frac{\alpha x^2}{1 + (1+\sigma_1)x^2 + \sigma_2x^4} - \gamma x + 1. \tag{2.15}$$

(a)   (b)

Figure 2.9. *(a) For some parameter ranges, the model by Hasty et al [4] of Eqn. (2.15) has two stable and one unstable steady, and hence displays bistability. Here* $\gamma = 15, \alpha = 50, \sigma_1 = 1, \sigma_2 = 5$. 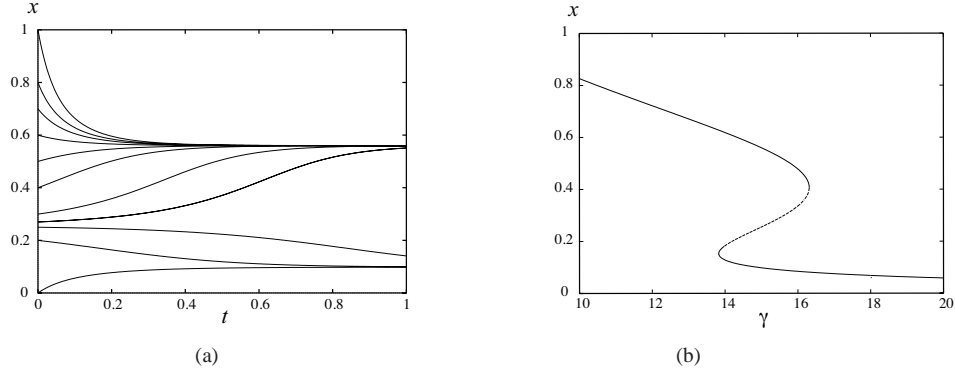*(b) Bifurcation diagram produced by Auto, with the bifurcation parameter* γ. *See XPP file and instructions in Appendix A.F.*

Here α is a (scaled) magnitude of the transcription rate due to repressor binding, and γ is a (scaled) turnover rate of the repressor. In general, the value of α would depend on the transcription rate and the DNA binding site concentration, whereas γ is an adjustable parameter that Hasty et al. manipulate.

In Fig. 2.8, we plot separately the two functions on the RHS of Eqn. (2.15) given by

$$f_1(x) = \frac{\alpha x^2}{1 + (1 + \sigma_1)x^2 + \sigma_2 x^4} \quad \text{(sigmoid curve)}, \quad f_2(x) = \gamma x - 1 \quad \text{(straight line)} \quad (2.16)$$

for three values of the slope γ. It is evident that the value of γ determines the number of intersection points of the sigmoid curve and the straight line, and hence, also the number of steady states of Eqn. (2.15). When γ is large (e.g. steepest line in Fig 2.8), the two curves intersect only once, at a low values of x. Consequently, for that situation, very little repressor protein is available. As γ decreases, the straight line becomes shallower. Here we see again the classic situation of **bistability**, where three steady states coexist. The outer two of these are stable, and the middle is unstable [Exercise 2.8]. This graphical argument is a classic mathematical-biology modeling tool that reappears in many contexts. When three intersections occur, the amount of repressor available then depends on initial conditions: on either side of the unstable steady state, the value of x will tend to either the low or the high x steady state. This situation is also shown in the time plot produced by a full simulation, in Fig. 2.9(a). Finally, as γ decreases yet further, two of the steady states are lost and only the high x steady state remains.

From Fig. 2.9(a) we see that any initial value of x will be attracted to one of the two outer stable steady states. Indeed, the gene and its product act as a switch. We summarize this behaviour in the bifurcation plot of Fig. 2.9(b) with γ as the bifurcation parameter. We find that the presence of three steady states depends on the values of γ. The range $14 \leq \gamma \leq 16$ corresponds to switch-like behaviour. In Exercise 2.9, we consider how this

and other experimental manipulations of the λ repressor system might affect the observed behaviour, using similar reasoning and graphical ideas.

2.4   Models for the cell division cycle

SOme of the original literature includes [12, 20, 21]. Here we mostly discuss the theoretical paper by Tyson and Novak [19].
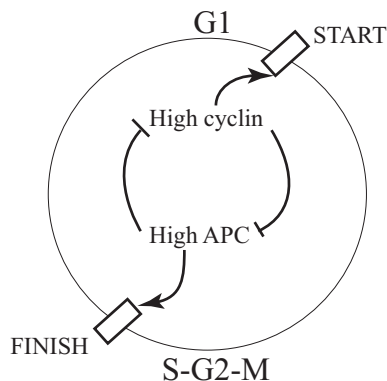

Figure 2.10. *The cell cycle and its check points (rectangles) in the simplified model discussed herein. The cycle proceeds clockwise from START. A high activity level of cyclin promotes the START and its antagonist, APC, promotes the FINISH part of the cycle.*

Cell division is conventionally divided into several phases. After a cell has divided, each daughter cell may remain for a period in a quiescent (non-growing) **gap** phase called G_0. Another, active (growing), gap phase G_1 precedes the S (**synthesis**) phase of DNA replication. The G_2 phase intervenes between S phase and M phase (**mitosis**). During M phase the cell material is divided. Here we will be concerned with two checkpoints of the cycle, after G1, signaling START cell division and after S-G2-M signalling FINISH the cycle (see Fig. 2.10.) Importantly, the START checkpoint depends on the size of the cell. This requirement is essential for a balance between growth and cell division, so that cells do not become gigantic, nor do they produce progeny that are too tiny. (In fact mutations that produce one or the other form have been used by Tyson *et al.* as checks for validating or rejecting candidate models.)

Control of the cell cycle is especially tight at the **checkpoints** mentioned above. For example, the division process seems to halt temporarily at the G_1 checkpoint to ascertain whether the cell is large enough to continue to progress through the cycle or whether a process other than mitosis is called for (e.g., terminal cell differentiation or the alternative "meiotic" path to cell division). Once this checkpoint is passed, the cell has irreversibly committed to undergoing division and the process must go on.

Regulation of the cell cycle resides in a network of molecular signaling proteins. At the center of such a network are kinases whose activity is controlled by **cyclin** To summarize, in phase G1 there is low Cdk and low cyclin levels (cyclin is rapidly degraded). START leads to induction of cyclin synthesis and buildup of cyclin and active Cdks that

persist during the S-G2-M phases. The DNA replicates in preparation for two daughter cells. At FINISH, APC is activated, leading to destruction of cyclin and loss of CdK activity. Then the daughter cells grows until reaching a critical size where the cycle repeats once more.

2.4.1 Modeling conventions

Before describing the simplest model for the cell cycle, let us collect a few definitions and conventions that will be used to construct the model. A number of these have been discussed previously, and we gather them here to prepare for assembling the more elaborate model.

Let C denote the concentration of a hypothetical protein participating in one of the reactions, and suppose that Q is the concentration of a regulatory substance that binds to C and leads to its degradation. Then the standard way to model the kinetics of C is

$$\frac{dC}{dt} = k_{\text{syn}}(\text{substrate}) - k_{\text{decay}}C - k_{\text{assoc}}CQ. \tag{2.17}$$

Here k_{syn} represents a rate of protein synthesis of C from amino acids, k_{assoc} is rate of association of C with Q, and k_{degrd} is a (basal) rate of decay of C.

Now suppose that some substance is simply converted from inactive to active form and back. Recall our discussion of activation-inactivation in Section 2.1.2. We consider the same ideas in the case of phosphorylation and dephosphorylation under the influence of kinases and phosphatases. We can apply the reasoning used for Eqn. (2.5) to write down our first equation. Moreover, scaling the concentration of C in terms of the total amount C_T [Exercise 2.3c] leads to

$$\frac{dC}{dt} = \frac{K_1 E_{\text{activ}}(1-C)}{J_1 + (1-C)} - \frac{K_2 E_{\text{deactiv}}C}{J_2 + C}. \tag{2.18}$$

Here J_1, J_2 are saturation constants, K_1, K_2 are the maximal rates of each of the two reactions and E_i are the levels of the enzymes that catalyze the activation/inactivation. Such equations and expressions appear in numerous places in the models constructed by the Tyson group for the cell division cycle.

2.5 Hysteresis and bistability in cyclin and its antagonist

An important theme in the regulatory network for cell division is that cyclin and APC are mutually antagonistic. As shown in Fig 2.11, each leads to the destruction (or loss of activity) of the other. To study this central module, Novak and Tyson considered the interactions of just this pair of molecules. This simplifying step ignores a vast amount of specific detail for clarity of purpose, but leads to insights in a modular approach promised above.

Let us use the following notation: Let Y (cYclin) denote the level of active Cyclin-Cdk dimers, and P, P_i the levels of active (respectively inactive) APC complex. It is assumed that the total amount of APC is constant, and scaled to 1, i.e. that $P + P_i = 1$. Then based on

Fig. 2.11 and the background of Section 2.4.1, the simplest model consists of the equations

$$\text{cyclin:} \qquad \frac{dY}{dt} = k_1 - (k_{2p} + k_{2pp}P)Y, \qquad\qquad (2.19a)$$

$$\text{APC:} \qquad \frac{dP}{dt} = \frac{V_i P_i}{J_3 + P_i} - \frac{V_a P}{J_4 + P}. \qquad\qquad (2.19b)$$
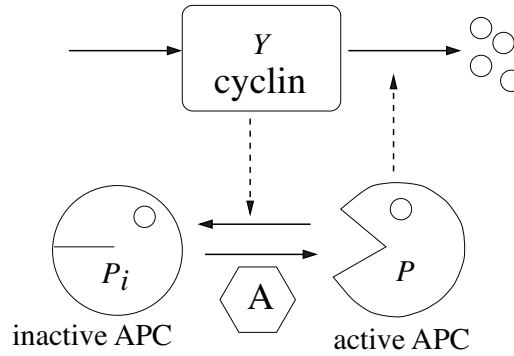
Figure 2.11. *The simplest model for cell division on which Eqs. (2.21) are based. Cyclin (Y) and APC (P) are mutually antagonistic. APC leads to the degradation of cyclin, and cyclin deactivates APC.*

The rates of the reactions are not constant. That is because a protein called here A, (and for now held fixed) is assumed to enhance the forward reaction, activating APC and cyclin (Y) enhances the reverse reaction, deactivating it. Tyson and Novak assume that:

$$V_i = (k_{3p} + k_{3pp}A), \quad V_a = k_4 mY.$$

Here, m denotes the mass of the cell, a quantity destined to play an important role in the model(s) to be discussed[2]. Recall that cell mass (for now considered fixed) is known to influence the decision to pass the START checkpoint. Thus, the model becomes

$$\frac{dY}{dt} = k_1 - (k_{2p} + k_{2pp}P)Y, \qquad\qquad (2.20a)$$

$$\frac{dP}{dt} = \frac{(k_{3p} + k_{3pp}A)P_i}{J_3 + P_i} - k_4 m \frac{YP}{J_4 + P}. \qquad\qquad (2.20b)$$

By conservation of the total amount of APC, and the scaling we have used,

$$P_i = 1 - P.$$

---

[2]The reader will note that cell mass m is introduced already in the simplest model as a parameter, and that as the models become more detailed, the role of this quantity becomes more important. In the final models we discuss, m is itself a variable that changes over the cycle and influences other variables. L.E.K.

Hence,

$$\frac{dY}{dt} = k_1 - (k_{2p} + k_{2pp}P)Y, \tag{2.21a}$$

$$\frac{dP}{dt} = \frac{(k_{3p} + k_{3pp}A)(1-P)}{J_3 + (1-P)} - k_4 m \frac{YP}{J_4 + P}. \tag{2.21b}$$

This constitutes the first minimal model for cell cycle components, and our first task will be to explore the bistability in this system.
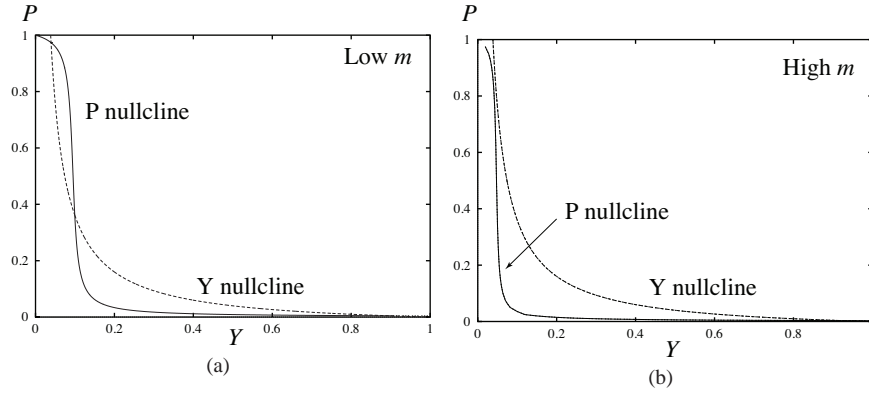

(a)

(b)

Figure 2.12. *The YP phase plane for Eqs.* (2.21) *and parameter values as shown in the XPP file in Appendix A.H.1. Parameters with units of 1/time are:* $k_1 = 0.04, k_{2p} = 0.04, k_{2pp} = 1, k_{3p} = 1, k_{3pp} = 10, k_4 = 35$, *Other (dimensionless) parameters are:* $A = 0, J_3 = 0.04, J_4 = 0.04$. *Here the cell mass is as follows:* (a) $m = 0.3$. *There are three steady states, a stable node at low Y high P (0.038, 0.96), a stable node at high Y low P (0.9,0.0045), and a saddle point at intermediate levels of both (0.1, 0.36).* (b) $m = 0.6$. *The nullclines have moved apart so that there is a single (stable) steady state at* $(Y, P) = (0.9519, 0.002)$: *this state has high level of cyclin, and very little APC.*

Figure 2.12 shows the typical phase-plane portrait of Eqs. (2.21), with the Y and P nullclines in dashed and solid lines, respectively. There are three steady states identified with the checkpoints at G1 and at S-G2-M. As the cell grows, its mass m increases. As shown in Fig. 2.12(a), this pushes the P nullcline to the left so that eventually, two points of intersection with the y nullcline disappear. (Just as this occurs, the saddle point and G1 steady state merge and vanish. This explains the term **saddle-node bifurcation** applied to such a transition, also called a **fold bifurcation**.) Parameter values of this model are provided in [19] and in the XPP file in Appendix A.H.1. We find that, at the bifurcation, transition to S-G2-M is very rapid once the GI checkpoint has been lost.

We show the bifurcation diagram for Eqs. (2.21) in Fig. 2.13(a), with cell mass m as the bifurcation parameter,. Then in Fig. 2.13(b), we identify steady states and the transition between them with parts of the cell cycle. We see the property of **hysteresis** that is characteristic of bistable systems: the parameter m has to increase to a high value to trigger the START transition, and then cell mass has to decrease greatly to signal the FINISH transition. Here the latter is associated with cell division at which m drops by a factor of 2.
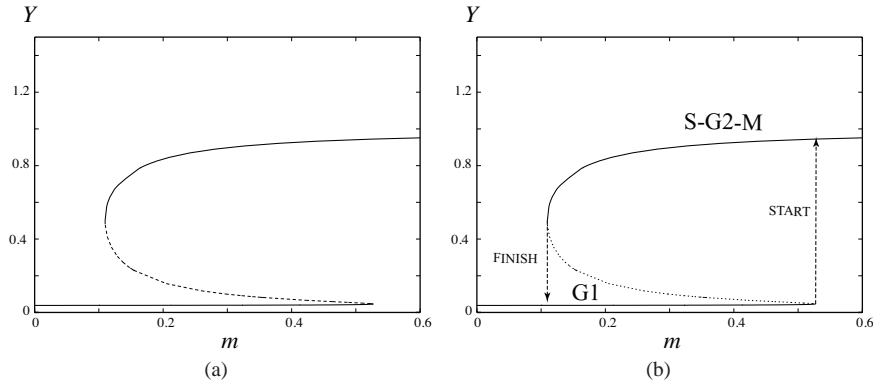
(a)   (b)

Figure 2.13. *(a) Bifurcation diagram for the simplest model of Eqs.* (2.21) *with cell mass m as the bifurcation parameter. The diagram was produced using XPP file in Appendix A.H.1. (b) Here we have labeled parts of the same diagram with corresponding phases of the cell cycle. Based on [19].*

2.6 Activation of APC

Up to now, the quantity A in (2.21b) has been taken as constant. A represents a protein called Cdc20 that increases sharply during metaphase (M) in the cell cycle. Next, Novak and Tyson assume that A is turned on in a sigmoidal kinetics by cyclin, leading to an equation with a Hill function of the form:

$$\frac{dA}{dt} = k_{5p} + k_{5pp}\frac{(mY/J_5)^n}{1+(Ym/J_5)^n} - k_6A. \tag{2.22}$$

The terms include some basal rate of production and decay, aside from the cyclin-dependent activation term.

Novak and Tyson first assume that the timescale of APC kinetics (and specifically of the Cdh1 protein in APC) is short, justifying a QSS assumption. That is, we take $P \approx P_{ss}(A,Y,z)$, i.e. P follows the other variables with dependence on a host of parameters here abbreviated by z,

$$P = P_{ss}(A,Y,z).$$

The details of the expression for P_{ss} are discussed in Exercise 2.10 and are based on the Goldbeter-Koshland function previously discussed. With this simplification, the equations of the second model are

$$\frac{dY}{dt} = k_1 - (k_{2p} + k_{2pp}P_{ss})Y, \tag{2.23a}$$

$$\frac{dA}{dt} = k_{5p} + k_{5pp}\frac{(mY/J_5)^n}{1+(Ym/J_5)^n} - k_6A. \tag{2.23b}$$

with P_{ss} as described above. We show a few of the *YA* phase plane portraits in Figure 2.14. It is seen that for small cell mass, there are three steady states: a stable spiral, a stable node, and a saddle point. All initial conditions lead to either one of the two stable steady

states. As *m* increases past 0.49, a small limit cycle trajectory is formed. That cyclic loop trajectory (shown in Fig 2.14(b)) is unstable, so trajectories are forced around it to either of the attracting steady states (one inside, and one close to the origin.). We show more details of the events close to this type of bifurcation in the schematic sketch in Fig. 2.16. When *m* increases further on, past $m = 0.8$, the saddle point and stable node formerly near the sharply bent knee of the *A* nullcline has disappeared. This means that the phase G1 is gone, replaced by a stable limit cycle that has grown and become stable. This type of bifurcation is a saddle-node/loop bifurcation. (See Fig. 2.17 for details.)
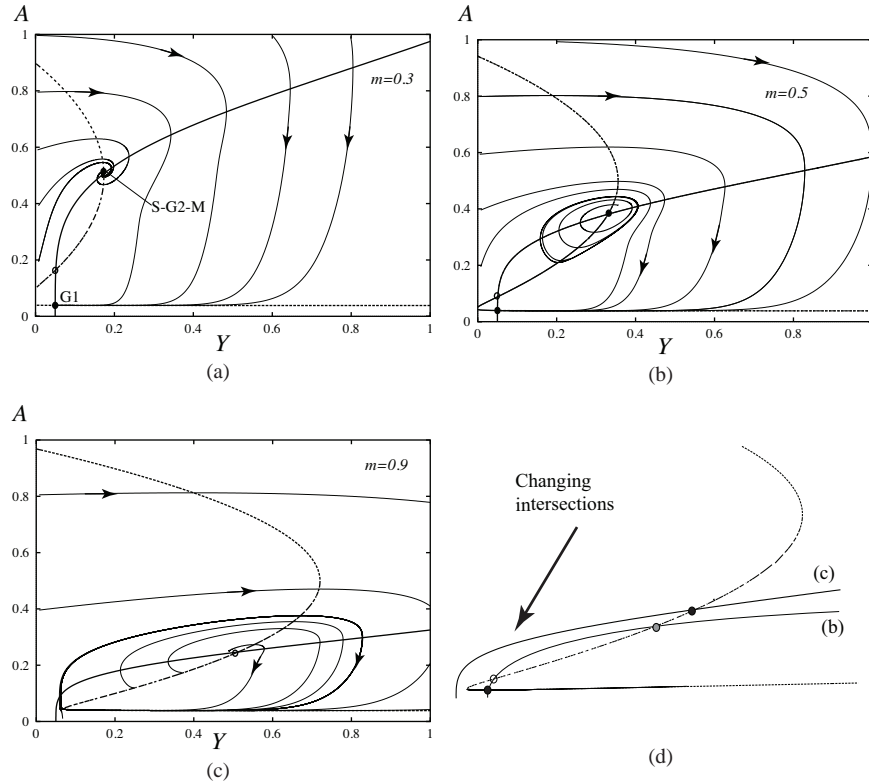
Figure 2.14. *The YA phase plane for the model* (2.23)*. The Y nullcline is the solid dark curve, and the A nullcline is the dashed curve. The steady states correspond to phases G1 and S-G2-M as labeled in (a). Phase plane portraits are shown for (a) m = 0.3, (b) m = 0.5 (Here there is an unstable limit cycle, that exists for 0.4962 < m < 0.5107. To plot this loop, we have set Δt as a small negative timestep, i.e. integrated backwards in time.) (c) m = 0.9: there is a large loop trajectory that has formed via a saddle-node/loop bifurcation. (d) Here we show only the nullclines (drawn schematically) and how their intersections change in the transition between parts (b) and (c) of the figure. Note that two intersections that occur in (b) have disappeared in (c).*

In the model of Eqs. (2.23), for a small cell, the phase G1 is stable. As we have

seen above, the growth of that mass eventually leads to "excitable" dynamics, where a small displacement from G1 results in a large excursion (Fig 2.14(b)) before returning to G1. When the mass is even larger, G1 disappears altogether and a cyclic behaviour ensues. However, this is linked to division of the cell mass so that m falls back to low level, reestablishing the original nullcline configuration and returning to the beginning of the cell cycle.

2.6.1   The three-variable YPA model

We are now interested in exploring the three-variable model without the QSS assumption on P. Consequently, we adopt the set of three dynamic equations

$$\frac{dY}{dt} = k_1 - (k_{2p} + k_{2pp}P)Y, \tag{2.24a}$$

$$\frac{dP}{dt} = \frac{(k_{3p} + k_{3pp}A)(1 - P)}{J_3 + (1 - P)} - k_4 m \frac{YP}{J_4 + P}, \tag{2.24b}$$

$$\frac{dA}{dt} = k_{5p} + k_{5pp}\frac{(mY/J_5)^n}{1 + (Ym/J_5)^n} - k_6 A. \tag{2.24c}$$

with the same decay and activation functions as before. We keep m, all k's and J's as constants at this point. The model is more intricate than that of (2.21), and the bifurcation
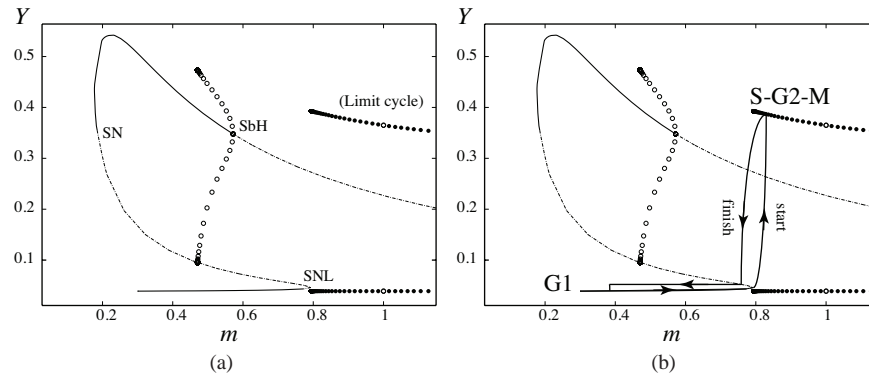
Figure 2.15. *(a) Bifurcation diagram for the full YPA model given by Eqs. (2.24) produced by the XPP file and instructions in the Appendix A.H.3. Bifurcations labeled on the diagram include a fold (saddle node, SN) bifurcation, a subcritical Hopf (SbH) and a saddle-node loop (SNL) bifurcation. The open circles represent an unstable limit cycle, as seen in Fig 2.14(b) of the QSS version of the model. The filled circles represent the stable limit cycle analogous to the one seen in Fig 2.14(c). (b) The course of one cell cycle is superimposed on the bifurcation diagram. The cell starts at the low cyclin state (G1) along the lower branch of the bistable curve. As cell mass increases, the state drifts towards the right along this branch until the SNL bifurcation. At this point a stable limit cycle emerges. This represents the S-G2-M phase, but as the cell divides, its mass is reset back to a small value of m, setting it back to G1.*

plot hence trickier to produce (but see instructions in Appendix A.H.3). However, with some persistence this is accomplished, yielding Figure 2.15[3].

Let us interpret Figure 2.15. In panel 2.15(a), we show the cyclin levels against cell mass m, the bifurcation parameter. (Cell mass increases along the lower axis to the right, as before.) Labeled on the diagram in 2.15(a) are several bifurcations (see caption), the most important being the saddle-node/loop bifurcation (SNL). Once cell mass grows beyond this critical value of $m \approx 0.8$, the lower G1 steady state disappears, and is replaced by a stable limit cycle. This is precisely the kind of transition we have already seen in Fig 2.14 (between the configurations in 2.14(b) and 2.14(c)).

Figure 2.15(b), we repeat the bifurcation diagram, but this time we superimpose a typical "trajectory" over one whole cell division cycle: the system starts in the lower right part of the diagram at G1, progresses to higher cell mass, passes the START checkpoint, duplicates DNA in the S-G2-M phase and then divides into two progeny, each of whose mass is roughly 1/2 of the original mass. This means m drops back to its low value for each progeny, and daughter cells are thereby back at G1.

$a < a_{\text{crit}}$ $a > a_{\text{crit}}$ $a >> a_{\text{crit}}$
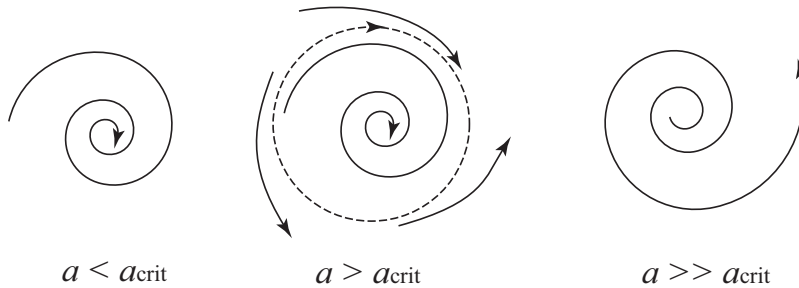
Figure 2.16. *Subcritical Hopf bifurcation. For a low value of some parameter a, the system has a stable spiral. Beyond some critical value, $a > a_{crit}$, an unstable limit cycle with some finite diameter suddenly appears. Then, as a continues to decrease, the limit cycle shrinks and vanishes, and the spiral becomes unstable. See also Fig* **??**.

To fix ideas we illustrate the two bifurcations in Figs 2.16 and 2.17. The first, Fig. 2.16, shows what happens in the phase plane as some parameter a goes through a **subcritical Hopf bifurcation**. (We have seen an example of this in Chapter **??**, Fig **??**; here we review this idea in the new context.) Note the sudden appearance of an unstable limit cycle with finite amplitude, that in general persists while shrinking in diameter for some range of the bifurcation parameter. Fig. 2.17 shows how a **saddle-node/loop** bifurcation can lead to the birth of a stable limit cycle, just as we have seen in the context of the model discussed above.

---

[3]This plot shares many features with a bifurcation diagram for the QSS version of Fig 2.14 (not shown), but with somewhat different bifurcation values. L.E.K.

$$a < a_{\text{crit}} \qquad\qquad a = a_{\text{crit}} \qquad\qquad a > a_{\text{crit}}$$

Figure 2.17. *Saddle-node/loop bifurcation here involves an unstable spiral and a saddle point. As some bifurcation parameter, a, changes, the transitions shown here take place. When $a = a_{crit}$, there is a heteroclinic trajectory that connects the saddle point to itself. For 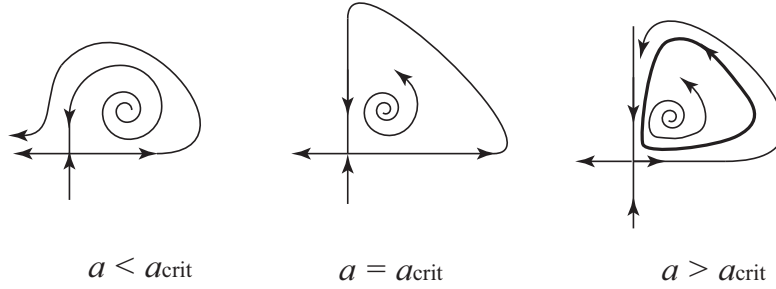larger values of a, a limit cycle appears and the heteroclinic loop disappears. At first appearance, the period of the limit cycle is very long ("infinitely long") due to the very slow motion along the portion of the trajectory close to the saddle point.*

2.6.2   A fuller basic model

The models considered so far have included only the skeletal forms of the regulatory cell division components. Including some additional interactions [19, p 255] results in a slightly expanded version suitable for describing the cell cycle of budding yeast. The notation for this model is provided in Table 2.1 and interactions between these are illustrated in Figure 2.18.

The equations are given by the following:

$$\text{cyclin:} \qquad \frac{dY}{dt} = k_1 - (k_{2p} + k_{2pp}P)Y, \tag{2.25a}$$

$$\text{APC:} \qquad \frac{dP}{dt} = \frac{(k_{3p} + k_{3pp}A_A)(1-P)}{J_3 + (1-P)} - k_4 m \frac{YP}{J_4 + P}, \tag{2.25b}$$

$$\text{Total A:} \qquad \frac{dA_T}{dt} = k_{5p} + k_{5pp}\frac{(mY/J_5)^n}{1 + (Ym/J_5)^n} - k_6 A_T, \tag{2.25c}$$

$$\text{Active A:} \qquad \frac{dA_A}{dt} = k_7 I_P \frac{A_T - A_A}{J_7 + A_T - A_A} - k_6 A_A - k_8[\text{Mad}]\frac{A_A}{J_8 + A_A}, \tag{2.25d}$$

$$\text{IEP:} \qquad \frac{dI_P}{dt} = k_9 mY(1 - I_P) - k_{10}I_P, \tag{2.25e}$$

$$\text{cell mass:} \qquad \frac{dm}{dt} = \mu m\left(1 - \frac{m}{m_s}\right). \tag{2.25f}$$

Eqs (2.25a) and (2.25b) for cyclin and APC have not changed since the previous model. As in the YPA three-variable model, APC is activated by the substance A (specifically Cdc20). However, we now distinguish between the active form, A_A, and the total amount, A_T of Cdc20. This protein is assumed to be inactive when first synthesized. The basal synthesis rate, shown as k_{5p} in (2.25c) is enhanced in the presence of high cyclin or when the cell mass is large (Hill function in the second term), as in the previous model.

Table 2.1. *Names of variables and their identity in the cell cycle models.*

Symbol	Identity	Activities and notes
Y	CyclinB	- controls Cdk kinases (binding partner) - high at START of cell cycle - antagonist of APC - when Y is low, cell divides.
P	Cdh1	- associated with APC (Anaphase promoting complex) - labels other proteins for destruction (including cyclin) - antagonist of cyclinB
A	Cdc20	- has an active form (A_A) and an inactive form - A_A acts as the activator for Cdh1 - A_T is total Cdc20.
I_p	IEP	- hypothetical activator of Cdc20 [19].
m	mass	- the mass of the cell - grows up to some maximal size if permitted - influences regulators of cell division - gets reset to low value once cell divides.

A turnover rate k_6 has been assumed. However, to exert its action, activation is required. The activated form of A, now denoted A_A is tracked in (2.25d). Note the resemblance of this equation to the form of a standard activation equation described previously in (2.4). The same turnover, at rate k_6 has been assumed for A_A as for A_T. The intermediates IEP activates A and Mad has the opposite effect on Cdc20 (Fig. 2.18), with Mad taken as a parameter in the model. (IEP is needed to get the right lag time, but was not identified with a specific molecule in [19].) The equation for IEP, (2.25e) has simple activation-deactivation, that are assumed to be affected by both cyclin and cell mass m.

Furthermore, from (2.25f) we see that cell mass is now a dynamic variable (rather than a parameter as before). The mass has a self-limited growth up to some maximal size m_s. (Compare with the form of a logistic equation and note that m increases whenever $m < m_s$ so long as case cell division does not occur.) A key further assumption is that a low value of Y causes cell division. A cell division event results in the mass of the cell being halved, and this occurs every time that the cyclin concentration falls below some threshold value (e.g. $Y_{thresh} = 0.1$).

As before, we here abandon hope of making analytical progress with a model of this complexity and turn to numerical simulations with parameter values obtained from [19] (See XPP code in Appendix A.H.4.) Simulations of the system (2.25) produce the figures
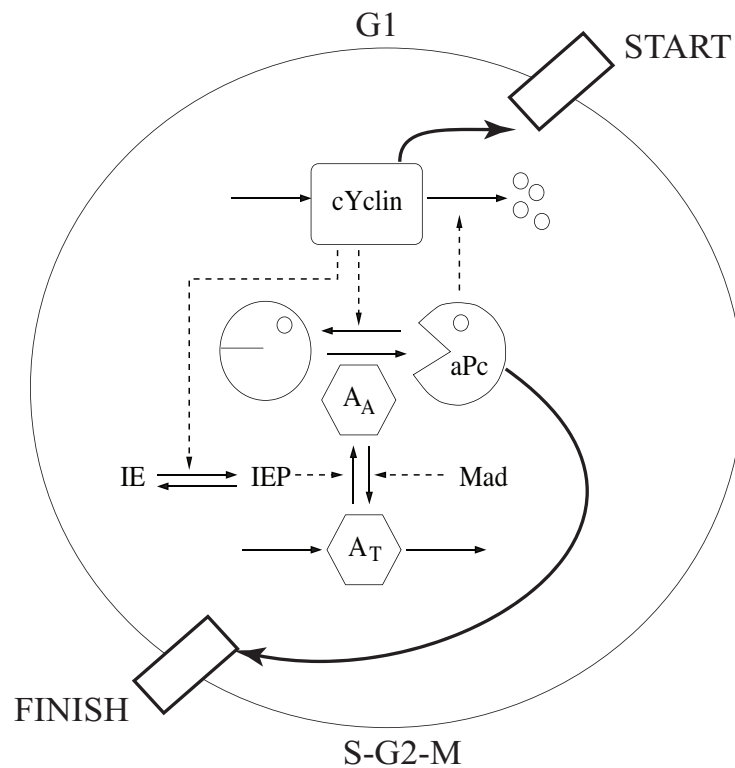
Figure 2.18. *The full model of the cell cycle depicted in Eqs.* (2.25)*. At its core is the simpler Y PA module, but other regulatory parts of the network have been added. See Table 2.1 for definitions of all components.*

shown in Fig 2.19. We note the following behaviour: At the core of the mechanism there is still the same antagonism between cyclin and APC: Now both vary periodically over the cell cycle, but they do so out of phase: APC is high when cyclin is low and vice versa. The total and active Cdc20, as well as the IEP shown in the third panel. Careful observation demonstrates that A_T cycles in phase cyclin, but activation takes longer, so that A_A peaks just as Y is dropping to a low level. A_A and I_P are in phase. Cell mass is a saw-tooth curve, with division coinciding with the sharp drop in cyclin levels.

Exercises

2.1. Suppose that $S, k_i > 0$ for $i = 0, 1, 2$ in Eqn. (2.1).

   (a) Find the solution $R(t)$ to this equation.

   (b) Find the steady state of the same equation.
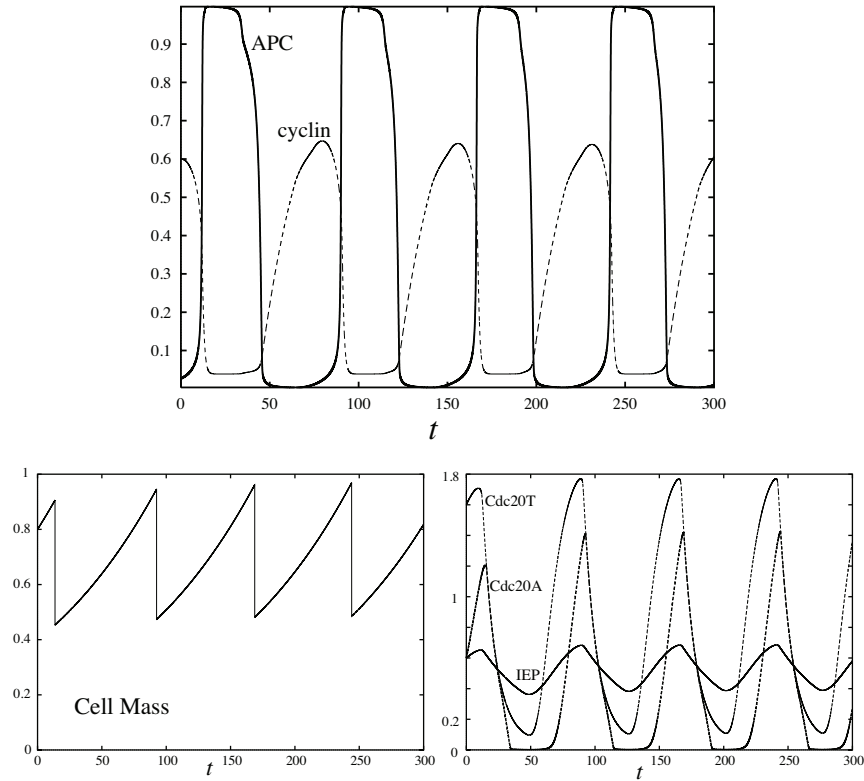
Figure 2.19. *Time behaviour of variables in the extended model of Eqs.* (2.25)*. Plots produced with the XPP file in Appendix A.H.4.*

    (c) Show that the steady state response depends linearly on the strength of the signal.

    (d) What happens if initially $S = 0$, and then at time $t = 0$ S is turned on? How can this be recast as an initial value problem involving the same equation?

    (e) Now suppose that S is originally ON (e.g. $S = 1$), but then, at $t = 0$, the signal is turned OFF. Answer the same question as in part (d).

    (f) Based on your responses to (d) and (e), what would happen if the signal is turned on at some time t_1 and off again at a later time t_2? Sketch the (approximate) behaviour of $R(t)$.

    (g) Create a simple XPP file and compare your answers to results of simulations.

2.2. Consider the simple phosphorylation-dephosphorylation model given by (2.2a). What is the analogous differential equation for R? Find the steady state concentration for R_p and show that it saturates with increasing levels of the signal S. [Hint: eliminate

R using the fact that the total amount, $R + R_p$ is conserved.] Assume that k_1, S, k_2 are all positive constants in this problem.

2.3. (a) Redraw Fig. 2.1 with parameters k_i labeled on the various arrows. Explain what are the assumptions underlying Eqn. (2.3). Show that conservation leads to (2.4).

   (b) What would be the corresponding equation for the unphosphorylated form R?

   (c) Rescale the variable R by the (constant) total amount R_T in Eqn. (2.4).

   (d) Solving for the steady state of the equation you got in part (c) leads to a quadratic equation. Write down that quadratic equation for $R_{p,SS}$. Show that your result is in the form of (2.7) (Once the appropriate substitutions are made).

   (e) Solve the quadratic equation, (2.7), in terms of the coefficients a, b, c, and then rewrite your result in terms of the parameters u, v, K, J. This (somewhat messy result) is the so-called Goldbeter-Koshland function.

   (f) According to Novak and Tyson [19], the Goldbeter-Koshland function has the form

$$G(u, v, J, K) = \frac{2\gamma}{\beta + \sqrt{\beta^2 - 4\alpha\gamma}}.$$

   for α, β, γ similar expressions of u, v, J, K. How does this fit with your result? Hint: recall that the an expression with radical denominator can be rationalized, as follows

$$\frac{1}{p + \sqrt{q}} = \frac{p - \sqrt{q}}{(p + \sqrt{q})(p - \sqrt{q})} = \frac{p - \sqrt{q}}{p^2 - q}.$$

2.4. Consider the adaptation module shown in Fig. 2.1c and given by Eqs. (2.8).

   (a) Show that the steady state level of R is the same regardless of the strength of the signal.

   (b) Is the steady state level of X also independent of signal? Sketch the (approximate) behaviour of $X(t)$ corresponding to the result for R and S shown in Fig. 2.2(b)

   (c) Use the XPP file provided in Appendix A.G.2 to simulate this model with a variety of signals and initial conditions.

   (d) How do the parameters k_i in Eqs. (2.8) affect the degree of adaptation? What if X changes very slowly? very quickly relative to R? (Experiment with the simulation or consider analyzing the problem in other ways.)

2.5. Here we consider Eqs. (2.8) using phase-plane methods, and assuming that S is constant.

   (a) Sketch the X and R nullclines in the XR plane.

   (b) Show that there is only one intersection point, i.e. a unique steady state, and that this steady state is stable.

   (c) Explain how the phase plane configuration changes when S is instantaneously increased, e.g. from $S = 1$ to $S = 2$.

2.6. Consider the genetic toggle switch by Gardner et al [3], given by the model equations Eqs. (2.11).

(a) Consider the situation that $n = 1$ in the repression term of the function (2.10) and in the model equations. Solve for the steady state solution(s) to Eqs. (2.11).

(b) Your result in (a) would have led to solving a quadratic equation. How many solutions are possible? How many (biologically relevant) steady states will there be?

(c) Consider the shapes of the functions I_x shown in Fig. 2.5. Using these shapes, sketch the nullclines in the phase plane for $n = m = 1$ and for $n, m > 1$. How does your sketch inform the dependence of bistability on these powers?

(d) Now suppose that $n = m = 3$ (as in Fig 2.6). How do the values α_i affect these nullcline shapes? Suppose α_1 is decreased or increased. How would this affect the number and locations of steady state(s)?

(e) Explore the behaviour of the model by simulating it using the XPP file in Appendix A.G.3 or your favorite software. Show that the configuration shown in Fig. 2.6 with three steady states depends on appropriate choices of the integer powers n, m, and comment on these results in view of part (c) of this exercise.

(f) Further explore the effect of the parameters α_i. How do your conclusions correspond to part (d) above?

2.7. Consider the genetic toggle switch in the situation shown in Fig. 2.6.

(a) Starting with $u = 2$, what is the minimal value of v that will throw the switch to v (i.e., lead to the high v steady state)?

(b) Fig. 2.6 shows some trajectories that "appear" to approach the white dot in the uv plane. Why does the switch not get "stuck" in this steady state?

(c) Suppose that the experimenter can manipulate the turnover rate of u so that it is $d_u = 1.5$ (rather than $d_u = 1$ and in (2.11)). How would this affect the switch?

2.8. Consider the chemical scheme proposed by Hasty et al [4] in (2.12).

(a) Write down the differential equations for the variables x, y, u, v, d corresponding to these chemical equations. (To do so, first replace the capitalized rate constants associated with the reversible reactions with forward and reverse constants (e.g. K_1 is replaces by κ_1, κ_{-1} etc).)

(b) Hasty et al assume that Eqs. (2.12a) are *fast*, i.e. are at quasi-steady state. Show that this leads to the following set of algebraic equations for these variables:

$$y = K_1 x^2, \tag{2.26a}$$
$$u = K_2 dy = K_1 K_2 dx^2, \tag{2.26b}$$
$$v = \sigma_1 K_2 dy = \sigma_1 K_1 K_2 dx^2, \tag{2.26c}$$
$$z = \sigma_2 K_2 uy = \sigma_2 (K_1 K_2)^2 dx^4. \tag{2.26d}$$

(c) Show that this QSS assumption together with the conservation equation (2.13) leads to the differential equation for x given by (2.14).

(d) Show that the equation you obtained in part (c) can be rewritten in the dimensionless form (2.15).

(e) Run the XPP code in Appendix A.F with the default values of parameters, and then change γ to each of the following values: (i) $\gamma = 12$ (ii) $\gamma = 14$, (iii) $\gamma = 16$, (iv) $\gamma = 18$. Comment on the number and stability of steady states.

(f) Connect the behaviour you observed in part (e) with the bifurcation diagram in Fig 2.9(b).

2.9. Consider the λ repressor gene model by Hasty et al [4], and in particular the model (2.15) discussed in the text. Suppose an experimenter carries out the following experimental manipulations of the system. State how the equation would change, or which parameter would change, and what would be the effect on the behaviour of the system. Use graphical ideas to determine the qualitative outcomes (The manipulations may affect some slope, height, etc. of a particular curve in Fig. 2.8.)

(a) The experimenter continually adds repressor at some constant rate to the system.

(b) The experimenter inhibits the turnover rate of repressor protein molecules.

(c) Repeat (b), but this time, the experimenter can control the turnover rate carefully and incrementally increases that rate from a low degradation level via intermediate level, to high level. What might be seen as a result?

(d) The experimenter inhibits the transcription rate in the cell, so that repressor molecules are made at a lower rate when the gene is active.

2.10. In the cell cycle model of Section 2.6, it is assumed that the variable P given by Eqn. (2.21b) is on quasi-steady state (QSS). Here we explore that relationship.

(a) Assume that $dP/dt = 0$ in (2.21b) and show that you arrive at a quadratic equation. Note similarity to Exercise 2.3d.

(b) Write down the solution to that quadratic equation.

(c) Show that you arrive at the Goldbeter-Koshland function, as in Exercise 2.3.

$$G(V_a, V_i, J_a, J_i) = \frac{2V_a J_i}{(V_i - V_a + V_a J_i + V_i J_a + \sqrt{(V_i V_a + V_a J_i + V_i J_a)^2 - 4(V_i - V_a)V_a J_i}}$$

2.11. Here we further explore the YP model of Eqs. (2.21) shown in Fig 2.12. Use the XPP file provided in Section A.H.1 (or your favorite software) to investigate the following:

(a) Replot the YP phase plane and add trajectories to the two diagrams shown in Figs. 2.12(a) and 2.12(a).

(b) Use your exploration in part (a) to determine the basin of attraction of each of the steady states in Figs. 2.12(a).

(c) Follow the instructions provided in Section A.H.1 to reproduce the bifurcation diagram in Fig. 2.13.

2.12. Consider the three variable YPA model for the cell cycle given by Eqs. 2.24

(a) Simulate the model using the XPP file provided Appendix A.H.3 (or your favorite software) for values of the cell mass in the ranges of interest shown in Fig 2.15, i.e. for low, intermediate, and larger cell mass. Sketch the time behaviour of Y,P,A for these simulations.

(b) Follow the instructions in Appendix A.H.3 to reproduce the bifurcation picture for this model.

2.13. Consider the following set of equations:

$$\frac{dx}{dt} = \alpha x - y - x(x^2 + y^2), \tag{2.27a}$$

$$\frac{dy}{dt} = x + \alpha y - y(x^2 + y^2). \tag{2.27b}$$

This set of equations represents the classic (supercritical) Hopf bifurcation, in which a stable limit cycle appears and gradually grow in diameter at a rate $\sqrt{\alpha - \alpha_{crit}}$.

(a) Explore this system numerically for a range of values of α to find its stable limit cycle.

(b) Now consider the related system that has a subcritical Hopf bifurcation

$$\frac{dx}{dt} = \alpha x - y + x(x^2 + y^2), \tag{2.28a}$$

$$\frac{dy}{dt} = x + \alpha y + y(x^2 + y^2). \tag{2.28b}$$

Study this system using the same methods and compare your results. You should find that an (unstable) limit cycle appears with nonzero diameter, and shrinks as the bifurcation parameter increases.

2.14. Use the XPP file provided in Appendix A.H.4 (or your favorite software) to simulate the model of Eqs. (2.25). Compare the time behaviour of APC and cyclin obtained in this model (e.g. in the first panel of Fig 2.19) with the corresponding behaviours obtained in the two and the three variable models.

includechapters/chapFEMCB

Chapter 3

Simple polymers

3.1 Simple models for polymer growth dynamics

3.1.1 Simple aggregation of monomers

We first look at simple aggregation where monomers can be added anywhere on the growing polymer. An example of this type could be highly branched polymer where every site is accessible for further addition, as shown in Fig 3.1. An example of this type was proposed by [11] to describe the aggregation of amyloid monomers into fibrils. Let us define the following variables:

$c(t)$ = number of monomer subunits in the volume at time t,

$F(t)$ = amount of polymer (in number of monomer equivalents) at time t,

$A(t)$ = total amount of material (in number of monomer equivalents) at time t.

(F is given a value that corresponds to the concentration of that much liberated monomer in the same reaction volume.)

Assume: The rate of growth depends on a product of c and F, with rate constant $k_f > 0$ (forward reaction rate) and the rate of disassembly or turnover is linearly proportional to the amount of polymer, with rate constant δ. Note that $A = c + F$ is constant [Exercise 3.1(a)]. Our model equations are then:

$$\frac{dc}{dt} = -k_f cF + \delta F, \tag{3.1a}$$

$$\frac{dF}{dt} = k_f cF - \delta F. \tag{3.1b}$$

Eliminating F by setting $F = A - c$ leads to a single equation for monomers:

$$\frac{dc}{dt} = (-k_f c + \delta)F = k_f (A - c)\left(\frac{\delta}{k_f} - c\right) \tag{3.2}$$
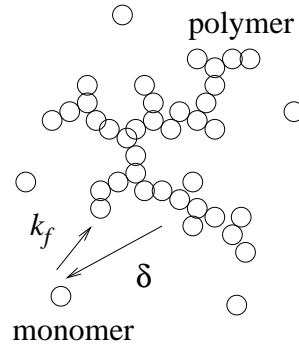
Figure 3.1. *A branched polymer. Any site on the polymer is competent for addition on new monomers. Hence the more polymer, the faster it grows for a given monomer concentration.*

It follows that there is a critical concentration of monomers, $c_{crit} = \delta/k_f$, that plays a role in the dynamics. Let us exploit this fact to write Eqn. (3.2) in the simpler form,

$$\frac{dc}{dt} = k_f(A - c)(c_{crit} - c).\tag{3.3}$$

Whenever $c < c_{crit}$, and $c < A$, the expression on the right hand side is positive so that dc/dt is positive. This implies that c increases in that case[4]. We cannot violate $c < A$ (so the term $(A - c)$ has to be positive), but if $c_{crit} < A$, then it is possible that $c_{crit} < c < A$. In that case, the product on the RHS of (3.3) is negative, and c decreases.

A plot of qualitative behaviour

In panels (a) and (b) of Fig 3.2, we plot dc/dt (on the vertical axis) versus c (on the horizontal axis) prescribed by Eqn. (3.3). In panel (b) of Fig 3.2, we show what happens in the case that $A < c_{crit}$.

The analysis so far has revealed that a non-trivial level of polymer occurs only if $A > c_{crit}$. In that case, the system evolves to $c(t) \to c_{crit}, F(t) \to A - c_{crit}$. We summarize several additional observations that can be made from simple examination of the form of Eqn (3.3) (without the need to fully solve this in closed form).

Steady state behaviour

Steady states of Eqn. (3.2) occur when $dc/dt = 0$. We observe that the amount of monomer left in solution is either

$$\bar{c} = c_{crit} = \frac{\delta}{k_f}, \quad \text{or} \quad \bar{c} = A.$$

---

[4]Recall that the **sign of the derivative** indicates whether a quantity is increasing or decreasing. Such arguments will be formalized and used insightfully in Chapter 1. L.E.K.
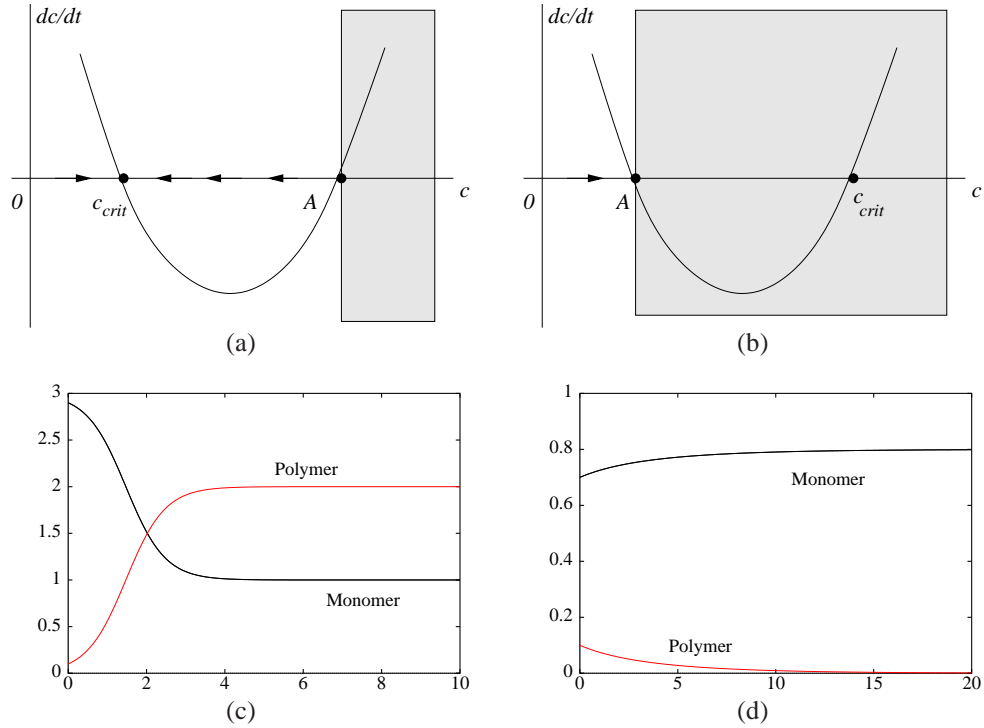
(a)   (b)

(c)   (d)

Figure 3.2. *Polymerization kinetics in simple aggregation. State space plots of (3.3) (also called phase portraits) showing monomer (c) and polymer (F) levels for constant total amount (A). (a) $A > c_{crit} = \delta/k_f$: in this case, c, will always approach its critical concentration, $\bar{c} = c_{crit} = \delta/k_f$, (b) $A < c_{crit}$: here there will be only monomers, and no polymers will form. The grey region is an irrelevant regime, since the level of monomer cannot exceed the total amount of material, A. Time plots of the two cases, produced by XPP (c) for $A > c_{crit}$, (d) for $A < c_{crit}$. Parameter values: $k_f = 1, \delta = 1, A = 3$. XPP code can be found in Appendix A.A.*

The amount of polymer at this steady state is (by conservation), $F \equiv \bar{F} = A - c_{crit} = A - \delta/k_f$, or $\bar{F} = 0$. Beyond the critical concentration, i.e. for $c > c_{crit}$, adding more monomer to the system (which thus increases the total amount A) will not increase the steady state level of monomer, only the polymerized form.

Initial rise time

The initial rate of the reaction, when the mixture just starts to grow: Suppose that initially, there is only a little bit of polymer to seed the reaction, i.e. $F(0) = \varepsilon$, $c(0) = A - \varepsilon \approx A$ for some small $\varepsilon > 0$. Then a good approximation of the polymer kinetics is given by substituting $c \approx A$ into the above equation to get

$$\frac{dF}{dt} \approx k_f(A - c_{crit})F = KF.$$

where $K = k_f(A - c_{crit})$ is a positive constant. Then the initial time behaviour of filaments, $F(t) = \varepsilon \exp(Kt)$, is exponentially growing provided $A > c_{crit}$.

Decay behaviour if monomer is removed

If the monomer is "washed away" from a mature reaction, i.e. effectively setting $c = 0$ in Eqn. (3.1b) leads to gradual disassembly of polymer, since then

$$\frac{dF}{dt} \approx -\delta F.$$

The polymer will decay exponentially with rate constant δ, i.e. $F(t) = F_0 \exp(-\delta t)$. This can be useful in determining values of parameters from data.

The full kinetic behaviour

Having identified main qualitative features of the system, and a few special cases such as early time behaviour, we turn to a full solution. Here we use software to numerically integrate the system of equations (3.1) and show the behaviour for a specific set of parameter values. We show this behaviour in panels (c) and (d) of Fig. 3.2. There are many software packages that can easily handle such differential equations. Here we use XPP (code provide in Appendix A.A).

Summary and observations

It is useful to gather the results of our simple analysis. We will find that such observations will help us later in distinguishing between one type of aggregation reaction and another.

3.1.2 Linear polymer growing at their tips

Here is a slightly different scenario, in which nucleation occurs only at some sites. For example, we consider a linear polymer with growth exclusively at the end(s) of the filaments, as shown in Fig 3.3. We keep the previous assumption that disassembly takes place by some bulk turnover of the polymer, i.e., not necessarily by monomer loss at the ends. We guide the reader through exploration of this case in Exercise 3.3, with main concepts summarized here more briefly.

We will define:

$n = $ Number of filaments (or filament tips) at which polymerization can occur.

We assume at this stage that the number of filament tips, n, is constant, and that neither breakage nor branching takes place. Then the appropriate model is

$$\frac{dc}{dt} = -k_f cn + \delta F, \tag{3.4a}$$
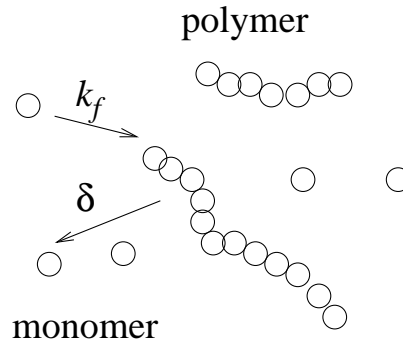
$$\frac{dF}{dt} = k_f cn - \delta F. \tag{3.4b}$$

Figure 3.3. *A linear polymer. Growth occurs at filament ends (on-rate k_f) and turnover takes place at rate δ.*

As before, conservation holds [Exercise 3.3a], and elimination of F leads to the monomer equation:

$$\frac{dc}{dt} = -k_f cn + \delta(A - c) = \delta A - c(k_f n + \delta). \tag{3.5}$$

The ratio $\delta/(nk_f)$ is dimensionless: it represents the ratio of the critical concentration to the concentration of tips.) However, properties of Eqs. (3.4) differ in several ways from that of our previous example.

Steady state

In Exercise 3.3c, we show that there is only one steady state, with monomer level

$$\bar{c} = \frac{\delta A}{k_f n + \delta} \equiv \beta A \quad \text{where} \quad \beta = \frac{\delta}{k_f n + \delta}. \tag{3.6}$$

The factor β so defined clearly satisfies $\beta < 1$ since $n, k_f > 0$. This means that such steady state exists in all cases, unlike the previous situation, in which it was contingent on a sufficiently high amount of material.

The linear structure and turnover kinetics of the polymer considered here has the following further implications: As shown in Fig 3.5, the ratio of polymer to monomer at steady state is constant. That ratio does not depend on the total amount of material, only on the reaction rates and the number of filament ends. Provided there are initial fiber ends on which to polymerize, growth of polymer occurs for any level of monomer. Increasing the total amount of material will increase both monomer and polymer proportionately. A large number of small filaments will grow to larger overall mass than a few long filaments, since more tips are available for polymerization.

One way to control the relative proportion of the polymerized form is to increase the number of "ends" at which polymerization occurs. This observation is germaine to actin, where specific agents lead to the creation of "new ends" at which polymerization occurs, or to the capping/uncapping of such ends to slow or accelerate polymerization.
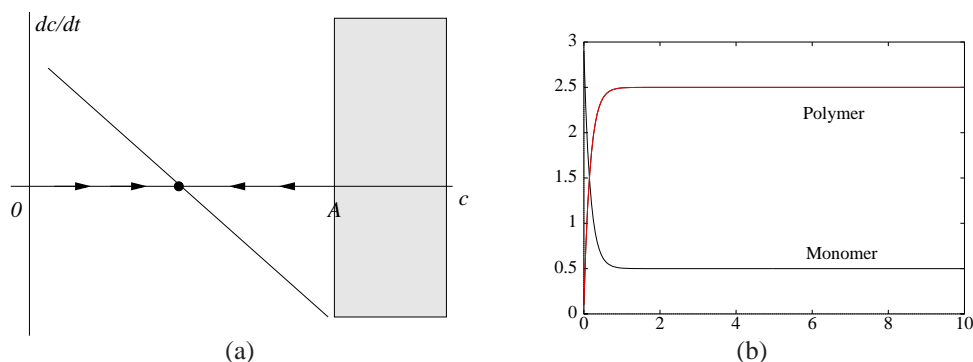
Figure 3.4. *Polymerization kinetics in filament elongation with growth occurring only at filament tips, given by Eqs.* (3.4). *Here the number of tips, n is assumed to be constant. (a) the flow is always towards a unique steady state, which is inside the domain. (b) time plot produced with XPP code (See Appendix A.B). Parameter values were $k_f = 1, \delta = 1, n = 5$ and initial conditions were $c(0) = 2.9, F(0) = 0.1$*
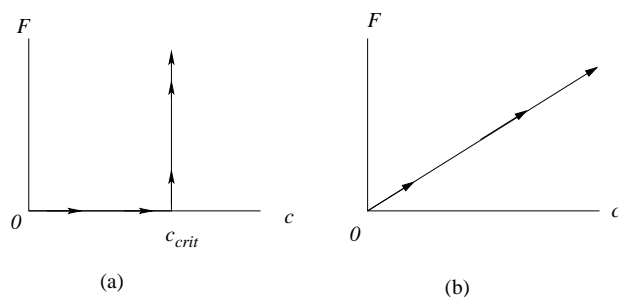

Figure 3.5. *Steady state values of polymer and monomer as the total amount of material A is slowly increased (direction of arrows). (a) In the case of simple aggregation, Eqs.* (3.1), *discussed in Section 3.1.1, for monomer concentration $c = c_{crit} \leq A$ no polymerization will occur. Thereafter, the monomer level will be constant and excess material will all be incorporated into polymer. (b) In a linear polymer with irreversible addition of monomer only at filament ends as in Eqs.* (3.4) *of Section 3.1.2, there will be a constant ratio of monomer and polymer. As A increases, both will increase. The slope of the line in (b) is nk_f/δ. Increasing the number of filament tips, n, will mean that more of the material is in polymer form.*

A comparison of the steady state behaviour of the two models thus far considered is given in Fig. 3.5. Here we show the distinct predictions for steady state behaviour for the two distinct polymer types as the total amount of material, *A* is gradually increased.

3.1.3 New tips are created and capped

New ends can be formed in a number of ways: (1) by spontaneous nucleation of filaments from monomers (2) by breakage of long filaments to produce shorter ones with more ends, or (3) by agents that lead to branching of the filaments. We here concentrate on the third mechanism.

Assume that the filaments sprout new tips at some constant rate, ϕ. This allows polymerization to accelerate. If new tips form without limit, no steady state will be possible. A control measure that limits explosive growth of new tips is needed, so we assume that the tips are capped at some rate κ. Kinetics of this type describe the polymerization of actin in presence of the nucleator Arp2/3 that leads to filament branching, and capping protein that stalls elongation at some tips [17]. Then the system of interest is

$$\frac{dn}{dt} = \phi F - \kappa n, \tag{3.7a}$$

$$\frac{dc}{dt} = -k_f c n + \delta F. \tag{3.7b}$$

where c is the monomer concentration $0 \leq c \leq A$ and F is filament length, as defined in Section 3.1.1. In Eqn. (3.7a) we see the creation of new tips along a filament (with rate ϕ per unit filament per unit time), and the first-order decay rate κn. In (3.7b) we have monomer being used up at each tip (fueling the extension of the filament) and being recycled from filament degradation. Note that tips do not carry a mass, as they are a site on an existing filament. The filament density equation is unchanged (here omitted), and F can be eliminated ($F = A - c$) as before leading to

$$\frac{dn}{dt} = \phi(A - c) - \kappa n, \tag{3.8a}$$

$$\frac{dc}{dt} = -k_f c n + \delta(A - c). \tag{3.8b}$$

This is a system of two differential equations in the variables $n(t), c(t)$. whose time behaviour is shown in the simulations of Fig 3.6. For low tip capping rate κ, the polymer will form, as in Fig 3.6(a). When κ is too high, the filaments initially start to grow, but eventually decay, as shown in Fig 3.6(b).

This system can also be studied in the cn phase plane (Figure 3.7(a,b).) It is evident that there are up to two steady states, $n = 0, c = A, F = 0$ (unstable) and a stable steady state at

$$\bar{c} = \frac{\delta}{k_f} \frac{\kappa}{\phi}, \quad F = A - \bar{c}, \quad n = \frac{\phi}{\kappa} F,$$

that is physically meaningful only if $A > \delta \kappa / k_f \phi$ (Fig. 3.7(a)). If this inequality is not satisfied, then only the trivial equilibrium is relevant and eventually, only monomer will remain (see Fig 3.7b and also Fig. 3.6b). In this sense, there exists an "effective critical concentration", whose value depends not only on the polymerization forward and back kinetics, but also on the creation and removal of tips that act as nucleation sites.
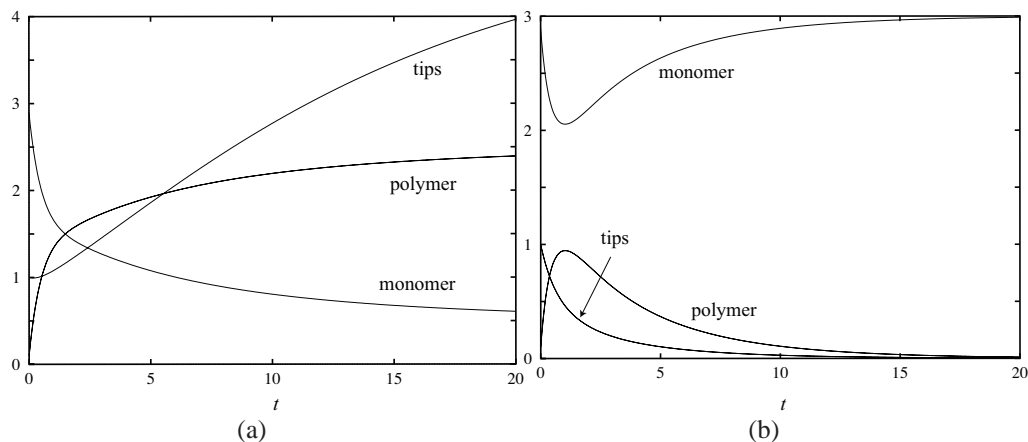
Figure 3.6. *Polymerization kinetics for the model* (3.8) *where new tips are created and capped. (a) For low capping rate, $\kappa = 0.1$ polymer is formed. (b) For $\kappa = 1$, the polymerization cannot be sustained, and eventually, only monomers are left. Other parameter values used were $k_f = 1, \delta = 1, \phi = 0.2, A = 3$. Simulations done with XPP file in Appendix A.D. See also Fig 3.7 for another way to plot the same information using a* **phase plane diagram**.
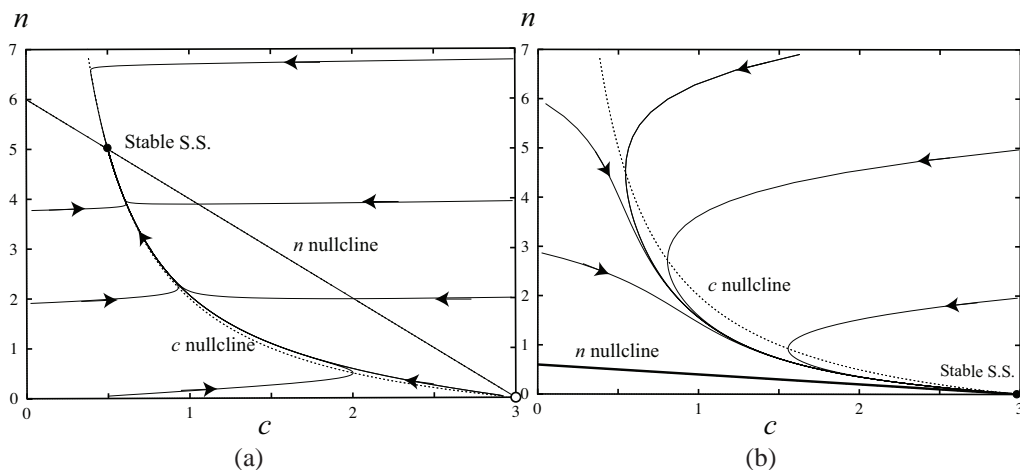
Figure 3.7. *Plane plots showing nullclines and steady states for the polymerization model in the case where filaments are broken to produce new tips, and tips are then capped. The horizontal axis is c, and the vertical axis is n. See Fig 3.6 for the corresponding time plots. (a): For low capping rate, $\kappa = 0.1$ polymer is formed. (b): $\kappa = 1$, the polymerization cannot be sustained, and eventually, only monomers are left. Other parameter values used were $k_f = 1, \delta = 1, \phi = 0.2, A = 3$. See Section A.D for XPP file that produced these phase plane diagrams.*

QSS on filament ends

If new tips are formed and removed rapidly relative to other kinetics, than a QSS on the variable n leads to $n \approx (\phi/\kappa)(A - c)$ so that

$$\frac{dc}{dt} = -k_f c n + \delta(A - c) = -k_f c \frac{\phi}{\kappa}(A - c) + \delta(A - c) = k_f(A - c)\left(\frac{\delta}{k_f} - \frac{\phi}{\kappa}c\right) \quad (3.9)$$

Thus, the dynamics of this case is similar to those discussed in Section 3.1.1 in the limit of rapid tip dynamics, but with a different "effective critical concentration", $c'_{crit} = \delta\kappa/(k_f\phi)$.

3.1.4   Initial dynamics

The initial behaviour of this system starting with $c \approx A$, and some $F = \varepsilon \neq 0$ depends on whether there are also exposed filament ends at $t = 0$. There are two possibilities:

Case A: Some exposed tips at $t = 0$: In Fig 3.6, we illustrate the case where $n(0) \neq 0$. In Exercise 3.10b we ask the reader to show that close to $t = 0$, filaments grow linearly and tips grow quadratically.

Case B: No exposed tips at $t = 0$: If tips are initially all capped so that $n(0) = 0$, then new tips must first form, before any polymerization can take place. In that case, close to $t = 0$, tips grow linearly and then filaments grow quadratically [Exercise 3.10c].

Implications

In this type of polymer reaction, with creation and capping of filament tips, either linear or quadratic initial polymerization rise time behaviour can occur. Washout decay is not changed from the description in Section 3.1.2. The effective critical concentration in such kinetics, $c'_{crit} = \delta\kappa/(k_f\phi)$, depends on turnover of both filaments and (exposed) tips, as well as branching and monomer on-rate. This means that any one of these parameters can influence the long-term behaviour.

Exercises

3.1.   (a) Show that the polymer equations (3.1) imply that the total amount of monomer and polymer are conserved.

   (b) Verify the equation for the rate of change of c obtained by eliminating F.

   (c) Explain how the diagram for dc/dt versus c is obtained from the differential equation for c.

3.2. Use the XPP file provided in Appendix A.A to explore the polymerization by aggregation discussed in Section 3.1.1. Show that you get results as in Fig 3.2. What parameter(s) or value(s) should you vary to get the cases shown in panels (c) and (d) of that figure?

3.3. (a) Show that the polymer equations (3.4) imply that the total amount of monomer and polymer are conserved.

 (b) Show that F can be eliminated from Eqn. (3.4a) to arrive at Eqn (3.5).

 (c) Show that (3.4) has a single steady state solution, and that the level of monomers at that steady state is given by (3.6). What is the corresponding level of polymer at that steady state?

 (d) Show that if the number of "tips", n, is constant, the steady state levels of monomer and polymer are proportional to each other.

3.4. Consider two special cases for the model (3.4) of polymer growing at n tips where $n > 0$ is constant.

 (a) First, consider the early time behaviour. Explain why this model implies that some polymer is needed initially so that further polymerization will occur.

 (b) Assume that close to the beginning of the reaction, $c \approx A$, and $F \approx \varepsilon$. Find the approximate behaviour of $F(t)$ at this early time. Show that $dF/dt \approx C$ so that F grows linearly with time.

 (c) What is the value of the constant C you found in part (b)?

 (d) Now consider the case that monomer is continuously removed from a polymerized mix that had been at its steady state. What will happen to the polymer?

3.5. Use the XPP code provided in Appendix A.B to explore the model for polymers growing at their tips discussed in Section 3.1.2. Show that you get the results given in Fig 3.4. How does the behaviour change if there are more tips ($n = 10$)? If the rate of growth is slower ($k_f = 0.2$) ?

3.6. Consider modifications of the model (3.4) as follows:

 (a) Show that if the polymerization at filament tips is reversible (with rate constant k_r for loss of monomer from tips), then this shifts the steady state to

$$\bar{c} = \frac{\delta A + k_r n}{k_f n + \delta}, \quad \bar{F} = A - \bar{c}. \tag{3.10}$$

 (b) Show that if filaments do not turn over as a whole, but rather add *and lose* monomers at their ends, then the kinetics are different. Explore this model by setting $\delta = 0$ and replacing $k_f cn$ by $(k_f c - k_r)n$ in the relevant equation.

 (c) Show that the revision in (b) introduces a critical concentration, $c_{crit} = k_r/k_f$.

3.7. Consider Eqn. (3.3). What are the units of each of the variables? Suppose we define new variables, $t^* = \delta t$ and $c^* = c/A$ where A is the total amount of monomer in the system. (Note that A, δ are positive constants carrying units. What are those units?)

 (a) Explain why the new variables, t^*, c^* are "dimensionless", i.e. are unit-less parameters.

 (b) Substitute $t = t^*/\delta, c = c^* A$ into Eqn. (3.2) and simplify the equations. Show that you obtain (after dropping the *'s).

$$\frac{dc}{dt} = (1 - \alpha c)(1 - c). \tag{3.11}$$

What is the value of the parameter α and what does it represent?

(c) Use the results of analysis of Eqn. (3.3) to draw conclusions about the behaviour of the dimensionless model, given by Eqn. (3.11).

3.8. For aggregating molecules, it may be the case that monomer addition or loss can only occur from the surface of a dense growing "pellet". This case is a variation on the theme described in the model (3.1) of Section 3.1.1. Here we examine this variant.

(a) Since the variable F has units proportional to mass, and assuming a 3D (roughly spherical) aggregate, show that the surface area of a single pellet would be proportional to $F^{2/3}$.

(b) Argue that this leads to the modified model

$$\frac{dc}{dt} = (-k_f c + \delta)F^{2/3} = k_f(A - c)^{2/3}\left(\frac{\delta}{k_f} - c\right).$$

(c) Show that the steady state monomer and polymer level is unchanged in this situation.

(d) Show that the initial growth (close to $t = 0$) and the "and washout kinetics" follow a power rather than exponential behaviour.

(e) Adapt the XPP code given in Section A.A to studying and characterizing the behaviour of this variant of the model.

3.9. Consider the model (3.8) for polymer filaments with tips that are created and capped.

(a) What is the corresponding differential equation for F?

(b) Find the steady state(s) of (3.8).

(c) Draw the qualitative state space plot (analogous to Fig. 3.2a,b) for c corresponding to the equation (3.9).

(d) For Eqn. (3.9), which steady state c is stable? (unstable?)

3.10. Consider the model (3.8) for polymer filaments with tips that are created and capped.

(a) Use the XPP file in Section A.D to simulate this model and recreate the time plots shown in Fig 3.6.

(b) If $n(0) \neq 0$, show that close to $t = 0$, filaments grow linearly and tips grow quadratically.

(c) If tips are initially all capped ($n(0) = 0$), show that close to $t = 0$, tips grow linearly and filaments grow quadratically.

Chapter 4

Introduction to nondimensionalization and scaling

This chapter is an introduction to the topic of dimensionless variables.

4.1 Simple examples

We start with simple models consisting of one differential equation in order to establish the motivation in an elementary setting. We first discuss the logistic population growth equation, and then move on to models in a chemical setting.

4.1.1 The logistic equation

A well-known model for the density-dependent growth of a population $N(t)$ is the **logistic equation** ,

$$\frac{dN}{dt} = rN\left(1 - \frac{N}{K}\right).$$

(4.1)

Here $r > 0$ is the **intrinsic growth rate** in units of 1/time, and $K > 0$ is the **carrying capacity**, in the same units as N. This equation is a limited-growth version of the **Malthus equation** discussed in Exercise 4.**??**.

Dividing both sides by K and regrouping terms leads to

$$\frac{1}{K}\frac{dN}{dt} = r\frac{N}{K}\left(1 - \frac{N}{K}\right), \quad \Rightarrow \quad \frac{d}{dt}\left(\frac{N}{K}\right) = r\frac{N}{K}\left(1 - \frac{N}{K}\right).$$

(4.2)

In this form, it is evident that N only appears in in the grouping N/K. We can simplify the equation and reduce the number of constants by treating this as a single new quantity. Accordingly, suppose we define a new variable,

$$y(t) = \frac{N(t)}{K}.$$

Note that in this form, the population is measured in "multiples" of the carrying capacity. Thus y is a pure number, a dimensionless variable carrying no units, even if originally we

had assigned units to N such as number of organisms per unit area of habitat. Making the substitution $N = Ky$ into Eqn (4.2) (or Eqn (4.1), for that matter), leads to the new equation,

$$\frac{dy}{dt} = ry(1-y). \tag{4.3}$$

We can go further with Eqn (4.3) and scale time so as to reduce the remaining parameter (r). To do so, we would define a new dimensionless variable $s = rt$. Then the substitution $t = s/r$ into Eqn (4.3) will eliminate the remaining parameter, leading to

$$\frac{dy}{ds} = y(1-y). \tag{4.4}$$

[Details in Exercise 4.1]. This elementary first example already illustrates that *introduction of dimensionless variables reduces the number of parameters that characterize a problem.* Observe that in Eqn. (4.4), there are no free parameters left. This means that we can understand the essential behaviour of such an equation by studying this single prototype rather than considering all possible results for multiple values of the parameters r, K for the unscaled version, Eqn (4.1). The behaviour of Eqn. (4.4) is explored in Section **??**.

4.2   Other Examples

We present a few additional examples and show how each can be nondimensionalized. Here we will also see steps to take when it is not immediately transparent which combinations of choices for scales are appropriate. Some of these examples arise in previous models (e.g. from Chapter 3) and others will be analyzed in later material.

Example 4.1 (Macrophages and dead cells). *Find a dimensionless formulation for the following set of equations arising in a model for macrophages ($m(t)$) removing dead cells ($a(t)$) and killing some cells in the process:*

$$\frac{dm}{dt} = g \cdot (M - m)a - km, \tag{4.5a}$$

$$\frac{da}{dt} = \kappa Cm - fma - da. \tag{4.5b}$$

Here M and C are total numbers of macrophages and target cells, respectively, assumed to be constant in this example, and given in units such as cells cm^{-3} (i.e. cells per cubic cm). Time t is measured in hours. g is the rate of activation of the macrophages by dead cell material, k is the rate of inactivation. κ is the rate of "bystander" killing of cells, f is the rate of removal of dead cells by macrophages and d is some other turnover of dead cell material. It is assumed that $g, k, \kappa, f, d > 0$ are constants. [See Exercise 4.3a for a discussion of the units of these parameters.]

Solution. We assume the following scalings:

$$m = \bar{m}m^*, \quad a = \bar{a}a^*, \quad t = \tau t^*.$$

Here $\bar{m}, \bar{a}, \tau$ are constant (dimension carrying) scales, to be chosen, and m^*, a^*, t^* are the numerical (dimensionless) variables. Then, substituting this into Eqs. (4.5) leads to

$$\frac{d(\bar{m}m^*)}{d(\tau t^*)} = g(M - \bar{m}m^*)\bar{a}a^* - k\bar{m}m^*, \tag{4.6a}$$

$$\frac{d(\bar{a}a^*)}{d(\tau t^*)} = \kappa C\bar{m}m^* - f\bar{m}m^*\bar{a}a^* - d\bar{a}a^*. \tag{4.6b}$$

We multiple both sides of Eqn. (4.6) by $\tau/\bar{m}$, and sides of Eqn. (4.8) by $\tau/\bar{a}$,

$$\frac{dm^*}{dt^*} = \frac{\tau}{\bar{m}} \left[g(M - \bar{m}m^*)\bar{a}a^* - k\bar{m}m^* \right], \tag{4.7a}$$

$$\frac{da^*}{dt^*} = \frac{\tau}{\bar{a}} \left[\kappa C\bar{m}m^* - f\bar{m}m^*\bar{a}a^* - d\bar{a}a^* \right]. \tag{4.7b}$$

Now distribute the terms and group constants and variable terms to obtain

$$\frac{dm^*}{dt^*} = g\bar{a}\tau((M/\bar{m}) - m^*)a^* - k\tau m^*, \tag{4.8a}$$

$$\frac{da^*}{dt^*} = \kappa C\frac{\bar{m}}{\bar{a}}\tau m^* - f\tau\bar{m}m^*a^* - d\tau a^*. \tag{4.8b}$$

Let us use square brackets to emphasize the groupings of constant terms:

$$\frac{dm^*}{dt^*} = [g\bar{a}\tau]([M/\bar{m}] - m^*)a^* - [k\tau]m^*, \tag{4.9a}$$

$$\frac{da^*}{dt^*} = \left[\kappa C\frac{\bar{m}}{\bar{a}}\tau \right] m^* - [f\tau\bar{m}]m^*a^* - [d\tau]a^*. \tag{4.9b}$$

We select values for the constant scale so as to simplify as many of these groupings as possible. In particular, we chose

$$[M/\bar{m}] = 1, \quad \left[\kappa C\frac{\bar{m}}{\bar{a}}\tau \right] = 1, \quad [d\tau] = 1.$$

This choice is, to some extent arbitrary in the current example. It implies that the convenient set of scales we have selected are

$$\bar{m} = M, \quad \tau = 1/d, \quad \bar{a} = \kappa C\bar{m}\tau = \frac{\kappa CM}{d}.$$

We now drop the *s. The equations then simplify to

$$\frac{dm}{dt} = \alpha(1 - m)a - \delta m, \tag{4.10a}$$

$$\frac{da}{dt} = m - \eta ma - a. \tag{4.10b}$$

where

$$\alpha = [g\bar{a}\tau], \quad \delta = [k\tau] = k/d, \quad \eta = [f\tau\bar{m}]. \tag{4.11}$$

In Exercise 4.3b we ask the reader to rewrite these quantities in terms of the original parameters of the problem and to interpret their meanings. ∎

Example 4.2 (Predator Prey equations). *Consider the following set of equations*

$$\frac{dx}{dt} = r_1 x \left(1 - \frac{x}{K}\right) - A\frac{xy}{D+x}, \tag{4.12a}$$

$$\frac{dy}{dt} = r_2 y \left(1 - \frac{y}{qx}\right). \tag{4.12b}$$

These equations have been used to model the dynamics of interacting prey $(x(t))$ and predators $(y(t))$. Assume that $r_i, K, A, D, q > 0$ are constants. Use dimensional analysis to reduce these to a dimensionless form.

Solution. We define the following scalings:

$$x = \bar{x}x^*, \quad y = \bar{y}y^*, \quad t = \tau t^*.$$

Here the quantities $\bar{x}, \bar{y}, \tau$ are convenient "scales" that will be chosen shortly, as in the previous example. They are constant, whereas the numerical values x^*, y^*, t^* that carry no dimensions are the variables. Substituting these assignments into Eqs. (4.12) leads to

$$\frac{d\bar{x}x^*}{d\tau t^*} = r_1 \bar{x}x^* \left(1 - \frac{\bar{x}x^*}{K}\right) - A\frac{\bar{x}x^* \bar{y}y^*}{D + \bar{x}x^*}, \tag{4.13a}$$

$$\frac{d\bar{y}y^*}{d\tau t^*} = r_2 \bar{y}y^* \left(1 - \frac{\bar{y}y^*}{q\bar{x}x^*}\right). \tag{4.13b}$$

We multiply both sides of Eqn. (4.13a) by $\tau/\bar{x}$ and both sides of Eqn. (4.13b) by $\tau/\bar{y}$ and simplify to obtain:

$$\frac{dx^*}{dt^*} = [r_1 \tau] x^* \left(1 - \left[\frac{\bar{x}}{K}\right] x^*\right) - \left[A\tau\frac{\bar{y}}{\bar{x}}\right] \frac{x^* y^*}{[D/\bar{x}] + x^*}, \tag{4.14a}$$

$$\frac{dy^*}{dt^*} = [r_2 \tau] y^* \left(1 - \left[\frac{\bar{y}}{q\bar{x}}\right] \frac{y^*}{x^*}\right). \tag{4.14b}$$

[See Exercise 4.4b.] We now make judicious choices that reduce the complexity of the terms. We can chose the scales $\bar{x}, \bar{y}, \tau$, i.e. we have three independent choices to make. It proves convenient to set

$$[r_1 \tau] = 1, \quad \left[\frac{\bar{x}}{K}\right] = 1, \quad \left[\frac{\bar{y}}{q\bar{x}}\right] = 1.$$

This is equivalent to selecting

$$\tau = r_1, \quad \bar{x} = K, \quad \bar{y} = q\bar{x} = qK.$$

The equations are thereby simplified to

$$\frac{dx^*}{dt^*} = x^* (1 - x^*) - \left[A\tau\frac{\bar{y}}{\bar{x}}\right] \frac{x^* y^*}{[D/\bar{x}] + x^*}, \tag{4.15a}$$

$$\frac{dy^*}{dt^*} = [r_2 \tau] y^* \left(1 - \frac{y^*}{x^*}\right). \tag{4.15b}$$

We drop the *'s and obtain the final dimensionless set of equations

$$\frac{dx}{dt} = x(1-x) - \alpha \frac{xy}{\delta+x} \tag{4.16a}$$

$$\frac{dy}{dt} = \nu y \left(1 - \frac{y}{x}\right) \tag{4.16b}$$

where the parameters in these have the following meanings:

$$\alpha = \left[A\tau\frac{\bar{y}}{\bar{x}}\right] = \frac{Aq}{r_1}, \quad \nu = [r_2\tau] = \frac{r_2}{r_1}, \quad \delta = [D/\bar{x}] = \frac{D}{K}.$$

In Exercise 4.4c, we discuss the meanings of these parameters. We also consider an alternate rescaling in part (d) of the same exercise. We will study this system further in a later chapter. (See Eqns. (??) and their analysis in Chapter ??.) ∎

Exercises

4.1. Consider the logistic equation (4.1).

  (a) Explain why it must be true that $N(t)$ and K have the same units.

  (b) Suppose $N(t)$ is in units of density of organisms (e.g. number per unit area) and time is measured in years. What are the units of the term dN/dt? of r? What are the units of the quantity $1/r$ and how could this be interpreted?

  (c) Now consider Eqn (4.3). Define a new variable $t^* = rt$ where r is the growth rate. Show that the substitution $t = t^*/r$ into Eqn (4.3) will eliminate the remaining parameter, leading to Eqn. (4.4). This is equivalent to rescaling time in units that have what meaning?

4.2. Suppose you have found a solution $y(t)$ to (4.4). Explain how you would convert this to a solution $N(t)$ to (4.1). [Hint: consider a back substitution using the relationships $s = rt$ and $y = N/K$.]

4.3. (a) For the model of macrophages and target cells given by (4.5), if m and c have units of cells cm^{-3} (i.e. cells per cubic cm) and time is measured in hours, what are the units for each of the parameters g, k, κ, f, d?

  (b) Determine the values of the dimensionless parameters α, δ, η from (4.11) in terms of the original parameters of the problem.

  (c) Interpret the meanings of these dimensionless ratios.

4.4. Consider the model for predator-prey interactions given by (4.12). Suppose predators and prey are both insects, and are measured in units of m^{-2} (e.g. number of individuals per square meter).

  (a) What are the units of the parameters r_i, K, A, D, q?

  (b) Verify the calculations resulting in (4.14).

  (c) Interpret the meanings of the dimensionless ratios α, ν, δ.

(d) Consider an alternate rescaling $\bar{x} = \bar{y} = K, \tau = 1/A$. Find the corresponding dimensionless equations and dimensionless parameter groupings. Interpret your results.

4.5. Consider the following equations for the growth of a single species of organism:

$$\frac{dP}{dt} = \frac{vP}{K+P} - dP. \tag{4.17}$$

(a) Interpret what these equations are saying.

(b) Define $x = P/\bar{P}, s = t/\tau$ where $\bar{P}, \tau$ are scales to be chosen. Use substitution to convert Eqn. (4.17) to a dimensionless form in terms of these scales.

(c) What is a reasonable choice for $\bar{P}$? For , τ? Are there more than one possible scalings that make sense for this model?

(d) Use an appropriate scaling to obtain a final dimensionless equations. What dimensionless parameter grouping(s) appear?

4.6. Consider the equation

$$\frac{dx}{dt} = ax - bx^3$$

(a) Show that this equation can be rescaled to the form

$$\frac{dx}{dt} = c\left(x - \frac{1}{3}x^3\right)$$

by defining an appropriate scale $\bar{x}$ for x.

(b) Show that by rescaling time, we arrive at a similar equation with $c = 1$.

See Section 1.0.1 for a further investigation of this cubic kinetics ODE.

4.7. Ludwig, Jones and Holling [9] studied the dynamics of the spruce budworm, here denoted $B(t)$. They suggested the following differential equation to describe the growth of these insects and predation by birds:

$$\frac{dB}{dt} = r_B B\left(1 - \frac{B}{K_B}\right) - \beta\frac{B^2}{\alpha^2 + B^2}. \tag{4.18}$$

(a) Explain the meanings of the terms in this equation.

(b) Rewrite these equations in dimensionless form. There are two choices for scales for the budworm density and two for time.

4.8. Hasty et al [4] derived a model for the concentration of a repressor $x(t)$ in the lysis-lysogeny pathway of the λ virus. A reduced version of this model is

$$\frac{dx}{dt} = \frac{AK_1K_2x^2}{1+(1+\sigma_1K_1K_2x^2+\sigma_2K_1^2K_2^2x^4)} - k_dx + r \tag{4.19}$$

Define a dimensionless repressor concentration $x^* = x\sqrt{K_1K_2}$ and a dimensionless time $t^* = t(r\sqrt{K_1K_2})$. Show that the dimensionless equation can be written in the form

$$\frac{dx}{dt} = \frac{\alpha x^2}{1+(1+\sigma_1x^2+\sigma_2x^4)} - \gamma x + 1. \tag{4.20}$$

Find the values of the parameters α, γ in terms of the original parameters.

Appendices

Appendix A

Appendix: XPP Files

Some instructions are provided here but readers who have never used XPP will find good resources for the installation and usage of this freeware in an online tutorial by Ermentrout, as well as in his written accounts. An extensive guide, with many other interesting examples, is [1]. A related text, also richly supported with XPP examples and instructions is [2].

A.A   Simulation for simple aggregation of monomers

ODE file for Fig 3.2 in Section 3.1.1

```
# actin1.ode
dc/dt=-kf*c*F +kr*F
dF/dt=kf*c*F -kr*F
param kf=1, kr=1
init c=0.7, F=0.1
done
```

A.B   Simulation for growth at filament tips

ODE file for Fig 3.4 in Section 3.1.2

```
# actin2.ode
dc/dt=-kf*c*n +kr*F
dF/dt=kf*c*n -kr*F
param kf=1, kr=1, n=5
init c=2.9, F=0.1
done
```

A.B.1   Cubic kinetics

The following file was used to produce the solution curves of Fig. 1.0.1 and the bifurcation diagram in Fig 1.4(b).

```
# cubic.ode
#
# The cubic first order differential equation
#
x'= c*(x-(1/3)*x^3+A)
param c=1,A=0
done
```

In order to produce the bifurcation diagram follow these steps: Run the .ode file with initial x value 1.5 and type "Initial condition" "Last" (I L) to continue the solution so that it is extremely close to its steady state value (repeat I L two or three times to do this). Type "File" "Auto" (F A). This opens a new window. Edit the panels as follows: **Parameter**: there is only one parameter, so this need not be changed. **Axes**: select "hI-lo". Then fill in the range Xmin = -2, Ymin= -3, Xmax=2, Ymax=3. **Numerics**: Change Par Min to -2, Par Max to 2, and Ds to 0.01. Press OK. **Run**: "Steady state". This will produce part of the diagram starting with the value of $A = 0$. To continue towards negative values of A, grab one of the points, and edit the Numerics panel to change Ds to -0.01. This will run the continuation in the opposite direction. For more details, see the book by Bard Ermentrout [1].

A.B.2   Pitchfork bifurcations

The following file was used to produce the pitchfork bifurcation shown in Fig. 1.9.

```
# Pitchfork.ode
x'=r*x-x^3
param r=-0.5
init x=0
done
```

Instructions: Run the file in auto for some time steps. Select F (File) A (Auto). The parameter will already be set to r, as that is the only parameter in the problem. Select Axes, hI-lo, and set Xmin:-0.1, Ymin:-1, Xmax: 0.25, Ymax 1. Select Numerics and change Par Min: -0.5, Par Max: 0.25. click OK, then Run: Steady state.

To produce the subcritical pitchfork bifurcation of Fig. 1.9, the file used was

```
# PitchforkSub.ode

x'=r*x+x^3

param r=0.2
init x=0
done
```

A.B.3   Transcritical bifurcation

To produce the transcritical bifurcation of Figure 1.8, the file used was:

```
# TRanscritBF.ode

x'=r*x-x^2

param r=0.2
init x=0.2
done
```

A.C   Systems of ODEs

A.D   Polymers with new tips

ODE file for Fig. 3.7

```
# TipsandCap.ode
#
# Simulation for formation of new filament tips
#
#
dc/dt=-kf*c*n +delta*(A-c)
dn/dt=phi*(A-c)-kappa*n
#
aux F=A-c
#dF/dt=kf*c*n -kr*(A-c)
param kf=1, delta=1, kappa=0.1, phi=0.2, A=3
init c=2.9, n=1
@ total=20,xp=c,yp=n,xlo=0,xhi=3,ylo=0,yhi=7
done
```

A.D.1   Limit cycles and Hopf bifurcations

The following file was used to make the bifurcation plot of a model that has a stable limit cycle.

```
# HopfBF.ode
# start at x=y=0
# start at r=0.5 and pick ds=-0.02 to first
# get the fixed pt. Then grab the HB point and
# pick ds=0.01 to get the Hopf.

x'=r*x-y-x*(x^2+y^2)
y'=x+r*y-y*(x^2+y^2)
```

```
param r=0.5
init x=0,y=0
done
```

The equations were integrated first with the above initial conditions. In Auto, the Numerics settings were changed as follows: ds: -0.02, Parmin:-0.5, Parmax: 2. Then select Run: Steady state. This produced the line of fixed point with bifurcation point at $r = 0$. The option Grab and tab key selects that bifurcation point. Hit Return. In the Numerics panel, switch to ds:0.01, then Run Periodic.

```
# HopfsubBF.ode
# start at x=y=0
# pick ds=-0.02 to get steady state
# then grab HB point and Run Periodic

x'=r*x-y+x*(x^2+y^2)
y'=x+r*y+y*(x^2+y^2)

param r=0.5
init x=0,y=0
done
```

Auto was run in a similar way, but the direction of steps ds need not be changed. The open dots signify an unstable limit cycle.

A.E   Fitzhugh Nagumo Equations

```
#FitzhughNagumo1.ode
# file to produce simulations for FHN model

dx/dt = c*(x-(x^3)/3-y+j)
dy/dt = (x+a-b*y)/c

aux v=-x

par j=0,a=0.7,b=0.8,c=3
# Consider either c=3 or c=10
# Parameters should satisfy  1-(2/3)b<a<1,    0<b<1

# Convenient initial conditions:
init x=2.0,y=2.0

@ total=20,xp=x,yp=y,dt=0.01,xlo=-3,xhi=2,ylo=-1,yhi=2
done
```

Now let us make the bifurcation diagram shown in Fig **??**. To do so, set $j = 0$ and integrate the equations to get as close as possible to the (stable) steady state. (e.g. use Initial

Conditions, Mouse [I M] to start close to the nullcline intersection, then continue using Initial Conditions, Last [I L] to get even closer. Start auto by clicking File, Auto [F A] and set the Axes to hI-Lo with Xmin:0, Ymin:-2,Xmax:1,Ymax:2. In the Numerics panel change Par Min:0 Par Max:1, click OK, and Run Steady state. You will get the horizontal branch of steady state, with a bifurcation point (HB). Grab that point and Run periodic (after decreasing ds to 0.005) to get this picture.

A.F   Lysis-Lysogeny ODE model (Hasty et al)

The following XPP file was used to produce Figs. 2.12 for the Lysis-Lysogeny model.

```
# lysislysogeny.ode
# Based on eq 7 in Hasty et al PNAS (2000) vol 97 #5 2075-2080
# should have a bistable switch
# gamma is the bifurcation parameter (range gamma= 14-16)
#
x'= alpha*x^2/(1+(1+sigma1)*x^2+sigma2*x^4)-gamma*x+1
param gamma=18,alpha=50,sigma1=1,sigma2=5
@total=10,xlo=0,xhi=10,ylo=0,yhi=1
done
```

To generate the bifurcation diagram[5], first integrate the ODE file starting from $x = 0$ a few times to get as close as possible to the steady state $x_{ss} = 0.06845$. (e.g., integrate, then "Continue" till $t = 500$, which does the job. Start Auto (File, Auto). Select Axes, hI-lo, Xmin:10, Ymin:0, Xmax:20, Ymax:1 [Note that gamma will be on the horizontal axis, and x_{ss} on the vertical axis.] Select Numerics, and change only Ds:-0.02, Dsmax:0.1,Par Min: 0, Par Max: 20. (Click OK.) Select Run, Steady state. This will produce the Bifurcation plot.

A.G   Simple biochemical modules

A.G.1   Production and Decay

The following XPP file was used to produce the production-decay behaviour in Fig. 2.2(a)

```
# ASProdDecay.ode
# Simple signal for production and decay of substance
#
R'=k0+k1*S-k2*R

# Signal gets turned on at time 0, off at time 3
# uses "Heaviside" step function to turn on or off

S=heav(t-0)-heav(t-3)
```

---

[5]I want to thank Bard Ermentrout for helping me with the Auto settings for this file. L.E.K.

```
param k0=1,k1=1,k2=1
init R=1
@total=10
done
```

A.G.2   Adaptation

The following XPP file was used to produce the adaptation behaviour in Fig. 2.2(b)

```
# AdaptTyson.ode
# An adaptation circuit
#
R'=k1*S-k2*X*R
X'=k3*S-k4*X

# Signal gets turned up in steps at times t=0, 5, 10, 15
# uses "Heaviside" step function

S=heav(t-0)+heav(t-5)+heav(t-10)+heav(t-15)

param k1=1,k2=1, k3=1, k4=2
init R=1, X=0.5
@total=10
done
```

A.G.3   Genetic toggle switch

The following XPP file was used to produce the switch-like behaviour of Fig. 2.6

```
# AToggleSwitch.ode
#
# Based on Gardner et al Nature (2000) Vol 403 pp 339-342
# By making either n or m large enough, get
# nonlinearity that produces multiple steady states
# and a switch-like response
#
u'=alpha1/(1+v^n)-u
v'=alpha2/(1+u^m)-v
param alpha1=3,alpha2=3,n=3, m=3
@ total=20,xp=u,yp=v,dt=0.01,xlo=0,xhi=4,ylo=0,yhi=4
done
```

A.H   Cell division cycle models

A.H.1   The simplest Novak-Tyson model (Eqs. (2.21))

The following XPP file was used to produce the phase plane of Fig 2.12 and the bifurcation diagram in Fig. 2.13.

```
# tysonCCJTB01.ode
# Model based on first system (eqs 2) shown in Tyson's paper
# JTB (2001) vol 210 pp 249-263
# Y=[CycB] = cyclin cdk dimers
# P=[Cdh1]= APN Cdh1 complex (proteolytic complex)
# Y and P are mutually antagonistic

Y'=k1-(k2p+k2pp*P)*Y
P'=Factiv(P)*(1-P)-Fdecay(Y,P)*P

Factiv(P)=(k3p+k3pp*A)/(J3+1-P)
Fdecay(Y,P)=k4*m*Y/(J4+P)

# parameters with units of 1/time:
par k1=0.04
par k2p=0.04,k2pp=1
par k3p=1,k3pp=10
par k4=35
par A=0

# mass of cell (try m=0.6, m=0.3)
par m=0.3

# Dimensionless parameters:
par J3=0.04,J4=0.04

@ dt=0.005
@ xp=Y,yp=P,xlo=0,xhi=1,ylo=0,yhi=1
done
```

To make an AUTO bifurcation diagram, the system was first started with the parameter $m = 0.1$, and integrated for many time steps to arrive at the steady state $y = 0.038684 p = 0.99402$. m was used as the bifurcation parameter. Auto Axes were set as hI-lo, with Y on the Y-axis, and Main Parm:m on the horizontal axis, and with Xmin:0, Ymin:0, Xmax:0.6, Ymax:1.5.

This system was slightly fiddly, and a few first attempts at producing a bifurcation diagram with the default AUTO numerics parameters were unsuccessful (MX type error).

AutoNumerics parameters were adjusted as follows: *Ntst:50*, Nmax:200, NPr:50, *Ds:0.002, Dsmin: 0.0001*, Ncol:4, EPSL:0.0001, Dsmax:0.5, *Par Min: 0.1, Par Max: 0.2*, Norm min:0, Norm Max: 1000, EPSU: 0.001, EPSS:0,001. The diagram was built up

gradually by increasing the range of the plotted curve.

A.H.2 The second Novak-Tyson model

The following file was used to simulate the *AY* phase plane plots in Fig 2.14(a)-2.14(c).
Note that here *P* is put on QSS.

```
# tysonCCJTB01_3QSSP.ode

# Model based on three eqns system (eqs 3) shown in Tyson's paper
# JTB (2001) vol 210 pp 249-263

# Y=[CycB] = cyclin cdk dimers
# P=[Cdh1]= APN Cdh1 complex (proteolytic complex)
# Y and P are mutually antagonistic
# A= Cdc14=Cdc20 - eqn (3) in this paper
# In this file we put P on QSS and look at Y and A


Y'=k1-(k2p+k2pp*P)*Y


#P'=Factiv(P)*(1-P)-Fdecay(Y,P)*P
#Factiv(P)=(k3p+k3pp*A)/(J3+1-P)
#Fdecay(Y,P)=k4*m*Y/(J4+P)


P=G((k3p+k3pp*A)/(k4*m),Y,J3,J4)

# Here is the Goldbeter-Koshland function that comes
# from solving dP/dt=0
G(Va,Vi,Ja,Ji)=2*Va*Ji/(Vi-Va+Va*Ji+Vi*Ja+ sqrt((Vi-Va+Va*Ji+Vi*Ja)^2-4*(Vi-Va)*Va*Ji))


A'=k5p+k5pp* ((m*Y/J5)^n)/(1+(y*m/J5)^n)-k6*A

# parameters with units of 1/time:
par k1=0.04
par k2p=0.04,k2pp=1
par k3p=1,k3pp=10
par k4=35
par k5p=0.005,k5pp=0.2,k6=0.1


# mass of cell (try m=1, m=0.3)
par m=0.3

# Dimensionless parameters:
par J3=0.04,J4=0.04,J5=0.3,n=4
```

```
@ dt=0.005
@ xp=A,yp=Y,xlo=0,xhi=1,ylo=0,yhi=1
done
```

A.H.3 The three-variable YPA model

The amended file below was used to produce Fig. 2.15 in Section 2.6.1.

```
#tyson.ode
# Equations

# Equations
Y'=k1-(k2p+k2pp*P)*Y
P'=(1-P)*(k3p+k3pp*A)/(J3+1-P)-P*k4*m*Y/(J4+P)
A'=k5p+k5pp* ((m*Y/J5)^n)/(1+(y*m/J5)^n)-k6*A

# Parameters with units of 1/time:
p k1=0.04
p k2p=0.04,k2pp=1
p k3p=1,k3pp=10
p k4=35
p k5p=0.005,k5pp=0.2,k6=0.1

# mass of cell (try m=0.6, m=0.3, m=1)
p m=1

# Dimensionless parameters:
p J3=0.04,J4=0.04,J5=0.3,n=4
# Numerics
@ TOTAL=2000,DT=.1,xlo=0,xhi=2000,ylo=0,yhi=6
@ NPLOT=1,XP1=t,YP1=Y
@ MAXSTOR=10000000
@ BOUNDS=100000
@ dsmin=1e-5,dsmax=.1,parmin=-.5,parmax=.5,autoxmin=-.5,autoxmax=.5
@ autoymax=.4,autoymin=-.5

# IC
Y(0)=1
P(0)=0.5
A(0)=0.1
done
```

To make the bifurcation diagram shown in Fig. 2.15, follow the procedure below.

- Change the integration method to "STIFF" (nUmerics, Method, Stiff, return, escape).

- First 'Initial condition', 'Go', we can get some periodic graph at the bottom of the drawing area. Click two peaks of the graph to find the approximate the period of the solution. It is about 56.45.

- 'numerics'—change 'total': 56.45, 'dt':0.05, escape.

- erase the original graph, 'IL' several time to make sure to get closer and closer to the exact stable period orbit.

- open the auto window. Select the auto settings as follows:
  'Parameter'—'Par1': m;
  'Axes'—'hilo'— 'Xmax': 30, 'Ymax': 5;
  'Numerics'—'Ntst':60,'Nmax':200,'Npr':500,'Epsl': 0.000001, 'ParMax':30;

- 'Run'—'Periodic', two short lines appears in the left bottom corner, if necessary, click 'abort' to stop them.;

- 'Grab' and enter.

- 'Numerics'—'Ds':-0.02.

- 'Run'—'extend', you will find the both two ends will extend, but it takes a long time, so if necessary, click 'abort' to stop them.

- Then we want to find the steady state. Before we do that, 'file'—'clear grab'.

- Go back to Xpp, 'Parameter'—m:10, and 'IL' several times.

- Go back to Auto, and 'Run'—'Steady State', a window will appear to ask you whether want to destroy the diagram, choose 'No', a fancy S-shaped graph will be added to the diagram (lighter than the original one).

- To see them more clearly, 'Axes'—'fit', 'redraw'. You might get a graph with some space between the first set of darker lines and lighter S-shaped curve, depending on how long you run before you click 'abort' when you run the extension.

- 'Axes'—'fit','redraw', the the former two darker line are averaged.

- There is more interesting behaviour for smaller values of m. To see these, click file, clear grab, and go back to XPP window. Change m to 0.3, and resimulate (Initial Cond, Go, I L,I L,I L, I L). Return to AUTO windo, and reset the numerics so that Parmin=0.3, Parmax = 2. Run. This will allow you to see the fold bifurction. There is also a subcritical Hopf bifurcation at $m = 0.5719$. You can see this by grabbing the Hopf point, adjusting the numerics menu to get Parmin=0.2, Parmax=0.6 and running the periodic.
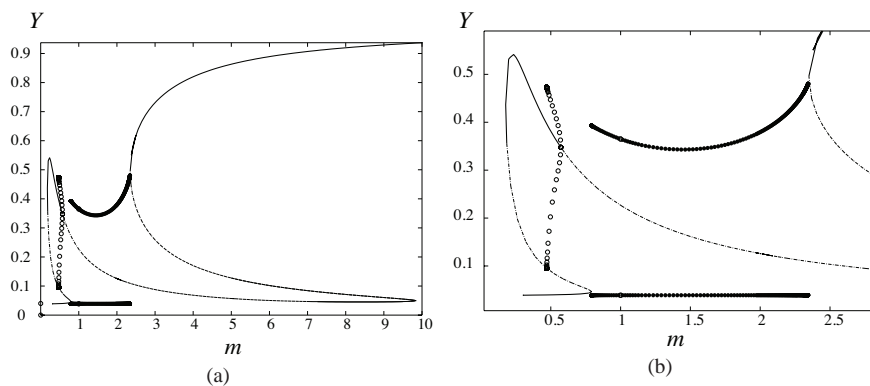
- The last graph is the same as 'Tyson.ps'.

Figure A.1. *Bifurcation diagram for the full YPA model given by Eqs.* (2.24) *(b) A zoom into part of the diagram of (a). See also Fig 2.15 for another zoomed view.*

A.H.4 A more complete cell cycle model

The file below was used to produce Fig 2.19. in Section 2.6.2.

```
# tysonCCJTB01_4.ode

# Model based on three eqns system (eqs 3) shown in Tyson's paper
# JTB (2001) vol 210 pp 249-263

# Y=[CycB] = cyclin cdk dimers
# P=[Cdh1]= APN Cdh1 complex (proteolytic complex)
# Y and P are mutually antagonistic
# A= Cdc14=Total Cdc20 - eqn (3) in this paper
#AA = active Cdc20 = Cdc20_A eqn (4)
# IP = [IAP]  eqn(5)

Y'=k1-(k2p+k2pp*P)*Y
P'=Factiv(P)*(1-P)-Fdecay(Y,P)*P

######NOTE: CHANGE IN THE FOLLOWING FORMULA A->AA
# as per Tyson's discussion on p 255

Factiv(P)=(k3p+k3pp*AA)/(J3+1-P)
Fdecay(Y,P)=k4*m*Y/(J4+P)


A'=k5p+k5pp* ((m*Y/J5)^n)/(1+(y*m/J5)^n)-k6*A

AA' = k7*IP*(A-AA)/(J7+A-AA) -k6*AA -k8*Mad*AA/(J8+AA)
```

```
IP'=k9*m*Y*(1-IP)-k10*IP

m'= mu*m*(1-m/ms)

# parameters with units of 1/time:
par k1=0.04
par k2p=0.04,k2pp=1
par k3p=1,k3pp=10
par k4=35
par k5p=0.005,k5pp=0.2,k6=0.1

par k7=1,k8=0.5,Mad=1
par k9=0.1,k10=0.02
par mu=0.01,ms=10

#Global flag: See XPP book p 36
# When Y falls below threshold, the cell divides,
# then its mass m is 1/2 its previous mass.
global -1 Y-Ythresh {m=m/2}
par Ythresh=0.1

# mass of cell (try m=0.6, m=0.3)
#par m=0.3

# Dimensionless parameters:
par J3=0.04,J4=0.04,J5=0.3,n=4
par J7=0.001,J8=0.001

init Y=0.6,P=0.02,A=1.6,AA=0.6,IP=0.6,m=0.8

@ dt=0.005,Total=300,MAXSTOR=500000,BACK= {White}
done
```

A.I   Odell-Oster model

The following XPP file can be used to investigate the Oster-Odell cell contraction model.

```
#Odell.ode
# file to produce simulations for Oster and Odell (1984) model

L'=k*(L0*1/(C^2+C0)-L)
C'=g*L-v*C+a*C^2/(b+C^2)

par k=1,L0=0.1,g=1,v=1,a=2.3,b=1.5,C0=0.5
@ total=20,xp=C,yp=L,xlo=0,xhi=2,ylo=0,yhi=0.3
done
```

Bibliography

[1] Bard Ermentrout, *Simulating, analyzing, and animating dynamical systems*, SIAM, Philadelphia, 2002.

[2] C.P. Fall, E.S. Marland, J.M. Wagner, and J.J. Tyson, *Computational cell biology*, Springer, New York, 2002.

[3] T.S. Gardner, C.R. Cantor, and J.J. Collins, *Construction of a genetic toggle switch in Escherichia coli*, Nature **403** (2000), no. 6767, 339–342.

[4] J. Hasty, J. Pradines, M. Dolnik, and JJ Collins, *Noise-based switches and amplifiers for gene expression*, Proceedings of the National Academy of Sciences of the United States of America **97** (2000), no. 5, 2075.

[5] P.A. Iglesias and A. Levchenko, *Modeling the cell's guidance system*, Science's STKE **2002** (2002), no. 148.

[6] B.N. Kholodenko, *Negative feedback and ultrasensitivity can bring about oscillations in the mitogen-activated protein kinase cascades*, European Journal of Biochemistry **267** (2000), no. 6, 1583–1588.

[7] ——— , *Cell-signalling dynamics in time and space*, Nature Reviews Molecular Cell Biology **7** (2006), no. 3, 165–176.

[8] A. Levchenko and P.A. Iglesias, *Models of eukaryotic gradient sensing: application to chemotaxis of amoebae and neutrophils*, Biophysical journal **82** (2002), no. 1, 50–63.

[9] D. Ludwig, D.D. Jones, and CS Holling, *Qualitative analysis of insect outbreak systems: the spruce budworm and forest*, The Journal of Animal Ecology **47** (1978), no. 1, 315–332.

[10] N.I. Markevich, J.B. Hoek, and B.N. Kholodenko, *Signaling switches and bistability arising from multisite phosphorylation in protein kinase cascades*, The Journal of Cell Biology **164** (2004), no. 3, 353.

[11] H Naiki and F Gejyo, *Kinetic analysis of amyloid fibril formation.*, Methods Enzymol **309** (1999), 305–318 (eng).

[12] B. Novak and J.J. Tyson, *Quantitative analysis of a molecular model of mitotic control in fission yeast*, J. theoret. Biol. **173** (1995), 283–305.

[13] G. Odell, G. Oster, P. Alberch, and B. Burnside, *The mechanical basis of morphogenesis. I. Ephitelial folding and invagination*, Dev. Biol. **85** (1981), 446–462.

[14] R.J. Prill, P.A. Iglesias, and A. Levchenko, *Dynamic properties of network motifs contribute to biological network organization*, PLoS biology **3** (2005), no. 11, 1881.

[15] H.M. Sauro and B.N. Kholodenko, *Quantitative analysis of signaling networks*, Progress in biophysics and molecular biology **86** (2004), no. 1, 5–43.

[16] S.H. Strogatz, *Nonlinear dynamics and chaos: With applications to physics, biology, chemistry, and engineering*, Westview Pr, 2000.

[17] T M Svitkina and G G Borisy, *Arp2/3 complex and actin depolymerizing factor/cofilin in dendritic organization and treadmilling of actin filament array in lamellipodia.*, J Cell Biol **145** (1999), no. 5, 1009–1026 (eng).

[18] J.J. Tyson, K. Chen, and B. Novak, *Sniffers, buzzers, toggles and blinkers: dynamics of regulatory and signaling pathways in the cell*, Current Opinion in Cell Biology **15** (2003), no. 2, 221–231.

[19] J.J. Tyson and B. Novak, *Regulation of the eukaryotic cell cycle: molecular antagonism, hysteresis, and irreversible transitions*, Journal of Theoretical Biology **210** (2001), no. 2, 249–263.

[20] J.J. Tyson, B. Novak, K. Chen, and J. Val, *Checkpoints in the cell cycle from a modeler's perspective*, Progress in Cell Cycle Res. (L. Meijer, S. Guidet, and H.Y.L. Tung, eds.), vol. 1, Plenum Press, New York, 1995, pp. 1–8.

[21] J.J. Tyson, B. Novak, G.M. Odell, K. Chen, and C.D. Thron, *Chemical kinetic theory: understanding cell-cycle regulation*, TIBS **21** (1996), 89–96.

Index